DNA renaturation at the water-phenol interface

A. Goldar[1,2,a] and J.-L. Sikorav[1,b]

[1] Groupe de Biophysique de l'ADN, CEA/Saclay, DBJC/SBGM, 91191 Gif-sur-Yvette Cedex, France
[2] Service de Physique des Etats Condensés, CEA/Saclay, DRECAM, 91191 Gif-sur-Yvette Cedex, France

Abstract. We study the renaturation of complementary single-stranded DNAs in a water-phenol two-phase system, with or without shaking. In very dilute solutions, each single-stranded DNA is strongly adsorbed at the interface at high salt concentrations. The adsorption of the single-stranded DNA is specific to phenol and relies on stacking and hydrogen bonding. We establish the interfacial nature of DNA renaturation at high salt, either with vigorous shaking (in which case the reaction is known as the Phenol Emulsion Reassociation Technique or PERT) or without it. In the absence of shaking, the renaturation involves a surface diffusion of the single-stranded DNA chains. A comparison of PERT with other known renaturation reactions shows that PERT is the most efficient one and reveals similarities between PERT and the renaturation performed by single-stranded nucleic acid binding proteins. The most efficient renaturation reactions (either with PERT or in the presence of condensing agents) occur in heterogeneous systems, in contrast with standard thermal renaturation, which takes place in the bulk of a homogeneous phase. This work highlights the importance of aromaticity in molecular biology. Our results lead to a better understanding of the partitioning of nucleic acids, and should help to design improved extraction procedures for damaged nucleic acids. We present arguments in favor of interfacial scenarios involving phenol in prebiotic chemistry.

PACS. 82.39.Pj Nucleic acids, DNA and RNA bases – 82.65.+r Surface and interface chemistry; heterogeneous catalysis at surfaces – 68.05.-n Liquid-liquid interfaces

1 Introduction

In 1977 Kohne, Levison and Byers [1] reported a striking experiment allowing a fast renaturation of complementary nucleic acids. They put denatured nucleic acids in an aqueous solution containing monovalent salts. Enough phenol was then added to obtain a second liquid phase. The constant and vigorous shaking of this biphasic system at room temperature created an instable emulsion in which the fast renaturation of the nucleic acids took place. They called this method the phenol emulsion reassociation technique or PERT. PERT accelerates RNA-RNA as well as RNA-DNA reactions, but is most efficient with DNA-DNA reactions at very low concentrations [1,2]. Under these conditions, the rate of DNA renaturation is independent of the length of the complementary strands, and is *"many thousand times faster than under the standard conditions"* [1]. The rate shows a weak temperature dependence, being only 3-4 times faster at 56 °C than at room temperature [1]. In addition, the rate depends on a critical manner on the salt concentration [3]. PERT has

been used with profit in many laboratories; it has allowed for instance Kunkel and coworkers [4] to isolate the gene responsible for the muscular dystrophy of Duchenne de Boulogne. The mechanism of PERT is still poorly understood. Kohne *et al.* [1] realized the possible physiological interest of such a system as well as its plausible prebiotic significance, but the lack of understanding of its basic mechanism seems to have precluded further investigations along these lines.

We have undertaken an experimental study of the behavior of nucleic acids in water-phenol two-phase systems, with the initial goal of clarifying the mechanism of PERT. We have hypothesized that PERT involves the coupling between two processes, single-stranded DNA (ssDNA) adsorption and annealing initiated at the water-phenol interface. We have therefore decided to study this reaction by using a decoupling scheme: instead of examining solely the behavior of the two complementary ssDNA chains obtained through the denaturation of a native double-stranded DNA (dsDNA) [1–3], we have chosen to investigate 1) the behavior of each ssDNA molecule in the absence of their complementary strand (with or without shaking) and 2) the renaturation of the

two complementary strands with various stoichiometries (again with or without shaking). Similar decoupling approaches have already been employed for related systems: DNA renaturation coupled with DNA aggregation in the presence of RecA protein [5]; DNA renaturation coupled with ssDNA folding [6,7] and DNA renaturation coupled with DNA aggregation in the presence of spermine [8].

In this work we use this decoupling scheme to investigate the partitioning and renaturation of very dilute ssDNA solutions in a water-phenol two-phase system. We first demonstrate that there is a salt-dependent adsorption of a single-stranded DNA molecule in the absence of its complementary strand at the water-phenol interface. The adsorption is essentially irreversible at high monovalent salt concentrations. In addition to phenol, we test thirteen other organic solvents for their ability to confine the single-stranded DNA at the water-solvent interface. Phenol turns out to be the most efficient solvent. We study the consequences of the gradual addition of an ssDNA in a high salt concentration water-phenol two-phase system where the complementary strand has been previously irreversibly adsorbed. We observe the progressive release of the adsorbed complementary strand in the aqueous phase, and show that this strand has renatured with the added ssDNA. This establishes the interfacial nature of the renaturation reaction in these conditions. We further investigate the effect of shaking on the rate of adsorption and renaturation. In the absence of shaking, adsorption is a slow, monomolecular diffusion-controlled process. The adsorption is completed within a few seconds if the solution is vigorously shaken. The study of DNA renaturation in the absence of shaking indicates the existence of a regime where the rate of the reaction depends on the two-dimensional diffusion of the two complementary single strands. We finally establish the interfacial nature of PERT, and determine the bimolecular rate of renaturation obtained with this technique. The measured value $(4.2 \times 10^{10}\,\mathrm{M}^{-1}\mathrm{s}^{-1})$ exceeds the rates obtained using either condensing agents or single-stranded DNA binding proteins (SSBPs).

These experimental studies have progressively led us to ponder on general questions dealing with both fundamental and applied biochemistry of nucleic acids. We will list briefly these questions, and examine them in the discussion section.

1.1 Adsorption and renaturation of DNA in the water-phenol two-phase system

What is the origin of the efficiency of phenol as a single-stranded nucleic acid binding and confining compound? What are the respective roles of hydrophobicity and aromaticity in the interaction of phenol and other simple organic compounds with nucleic acids [9–19]? What is the mechanism of the interfacial renaturation, with or without shaking?

1.2 Comparison with other renaturing approaches

How does the mechanism of this interfacial renaturation (with or without shaking) compare with the standard thermal renaturation approach [20–24], and with approaches involving condensing agents [3,8,25] or single-stranded binding proteins (SSBPs, often referred to as nucleic acid chaperones) [26–34]? What are the consequences of the coupling of the adsorption process with the coil-helix transition for the mechanism of this interfacial renaturation [35,36]? How does the interaction of phenol compare with the interaction of tyrosine and other aromatic amino acids of SSBPs with single-strand nucleic acids? In the absence of shaking, our results show the existence of an efficient two-dimensional diffusion process of the irreversibly adsorbed ssDNA chains. In a general manner, how can one obtain an efficient surface diffusion for nucleic acids or other polymeric chains?

1.3 Implications for the partitioning of nucleic acids in water-phenol and other two-phase systems

The purification of nucleic acids in two-phase systems (water-chloroform, water-phenol or water two-phase systems) is a common technique of molecular biology [37–45]. The partitioning of nucleic acids in water-phenol systems depends on numerous parameters: nucleic acid structure and conformation (double-stranded, single-stranded, denatured, supercoiled), nucleic acid concentration and sequence, pH, temperature, and salt concentration [40,46–51]. Losses of nucleic acids due to an "aggregation" at the water-chloroform or water-phenol interface or a transfer to the organic phase have been reported [51–55]. What is the role of surface phenomena in the partitioning of single and double-stranded nucleic acids?

1.4 Implications for the evolution of biological chemistry

Phenol is known to be a plausible prebiotic compound (see for instance [56] and further references therein). Furthermore, phenol is a very efficient nucleic acid binding and confining compound. This raises the possibility that phenol was an active compound in an early nucleic acid world [57–59]. What could have been the role of phenol and phenolic compounds in prebiotic chemistry and in the early stages of life? Surface phenomena, in particular adsorption on solid surfaces such as clays or other mineral surfaces are thought to have had an important role in prebiotic chemistry [60–64]. Could mechanisms involving an adsorption at a liquid-liquid interface [65] have also contributed to prebiotic chemistry?

2 Materials and methods

2.1 DNA

Two synthetic complementary 118 base-long single-stranded DNAs denoted 118+ (MW = 36318.3 Da) and

118− (MW = 36477.4 Da) were obtained from Eurogentec. The sequence of 118+ corresponds to the sequence of the nucleotides 4760–4877 of the plus strand of ϕX 174 [66] (positions 4758 and 4876 correspond to restriction sites for the enzyme *Hae* III).

2.2 Phenol and other organic solvents

Phenol (Molecular Biology grade) was obtained from Sigma and stored at $-20\,^{\circ}$C. We used a modification of the protocol described in [43] to prepare a water-phenol solution with a phenolic pH greater than 7.8. Phenol was melted at $68\,^{\circ}$C , and an equal volume of 0.5 M Tris-HCl (pH 8) at room temperature was added to it. The mixture was shaken at room temperature for 15 minutes and left at rest to separate the two phases. The organic phase was then collected using a separating funnel. This process was repeated with an equal volume of 0.1 M Tris-HCl (pH 8), until the pH of the phenolic phase (measured using a pH meter calibrated for aqueous solutions) exceeds 7.8 (this required at least two more extractions). When the proper pH was obtained (usually 7.85), the aqueous phase was removed and replaced by one volume of 0.1 M Tris-HCl (pH 8). This solution was kept at $4\,^{\circ}$C and used within a month. We did not add 8-hydroxyquinoline [39], because the presence of this compound modifies the partitioning of ssDNA in the water-phenol two-phase system (data not shown).

Dodecane, carbon tetrachloride, chloroform and benzylalcohol were obtained from Merck; chlorobenzene, fluorobenzene, iodobenzene and guaiacol (2-methoxyphenol) from Aldrich; aniline and bromobenzene from Fluka; 1-butanol from Prolabo; dichloromethane from SdS, and toluene from Sigma.

2.3 Plasticware

The experiments described in this work were performed at extremely low ssDNA concentrations (typically with a chain concentration in the 1–100 picomolar range). Low DNA concentrations together with high salt concentrations can lead to a significant adsorption on the walls of the tube if no precautions are taken. To prevent this effect, all experiments were carried out in 1.7 ml low-binding microcentrifuge tubes (Marsh Biomedical Products) coated with a methyl brush as follows: the tubes were filled with a solution of 2% dimethyldichlorosilane in (1, 1, 1)-trichloroethane (BDH). After at least 6 hours of incubation, the silane solution was removed and the tubes were thoroughly rinsed with a TE buffer (10 mM Tris-HCl (pH 7.5), 1 mM EDTA). In the water-phenol system, the adsorption of ssDNA on the walls of these coated tubes (determined as explained below) is always less than 6% of the total amount of ssDNA present in the tube at all salt concentrations between 0 and 3 M.

2.4 DNA labeling

The ssDNA 118+ and 118− were 5′-end labeled with T4 polynucleotide kinase using $\gamma\,^{32}$P-ATP (> 5000 Ci/mmol, AmershamPharmaciaBiotech) to a specific radioactivity of about 10^8 cpm/μg. The labeled ssDNAs were separated from unincorporated $\gamma\,^{32}$P-ATP by gel filtration on a Sephadex-G50 column (Nick Column, Pharmacia) equilibrated in a TE buffer (10 mM Tris-HCl (pH 7.5), 1 mM EDTA). The amount of unincorporated $\gamma\,^{32}$P-ATP still present in the solution of labeled ssDNA after the gel filtration was determined by an autoradiography of a sample submitted to a separation by gel electrophoresis as described below. The unincorporated $\gamma\,^{32}$P-ATP accounted for 5% or less of the total radioactivity present in the solution of labeled ssDNA.

2.5 Partitioning experiments involving vortexing

Unless stated otherwise, all partitioning experiments involving vortexing were performed as follows. The labeled ssDNA (160 μl containing the labeled ssDNA at a chain concentration of 125 pM (about 0.58 ng) in a TE buffer with various concentrations of NaCl) was added in a tube containing 40 μl of the phenolic phase prepared as explained above. This biphasic system was vortexed for 20 s at 2400 rpm (rounds per minute). The emulsion was then centrifuged at $15000 \times$ g for 1 min. After centrifugation, 100 μl of the aqueous phase and 10 μl of the organic phase were removed and their radioactivity was determined by scintillation counting. Direct Cerenkov counting was generally used for both types of samples (aliquots of aqueous or organic phases). We checked the reliability of these measurements for the organic phases by adding a scintillation cocktail (Pico-Fluor 40, Packard) to the aliquot and counting again. For phenol only, we also determined the amount of radioactivity adsorbed on the tube, by adding 1 ml of a TE solution containing the same NaCl concentration to the tube containing the rest of the two-phase mixture (60 μl of aqueous phase and 30 μl of organic phase: this yields a homogeneous liquid phase). The tube was vortexed for 20 s, the liquid phase removed and the radioactivity still bound to the walls of the tube was determined.

2.6 Renaturation experiments

The products of the renaturation experiments were separated by gel electrophoresis on a 15% polyacrylamide gel. The gel was dried and the quantities of single and double-stranded DNA as well as of unincorporated $\gamma\,^{32}$P-ATP were determined using a Phosphor Imager (Molecular Dynamics).

3 Results

3.1 Partitioning of ssDNA in the water-phenol system

Figure 1 shows the partitioning of the ^{32}P-labeled ssDNA 118− in the water-phenol two-phase system as a function
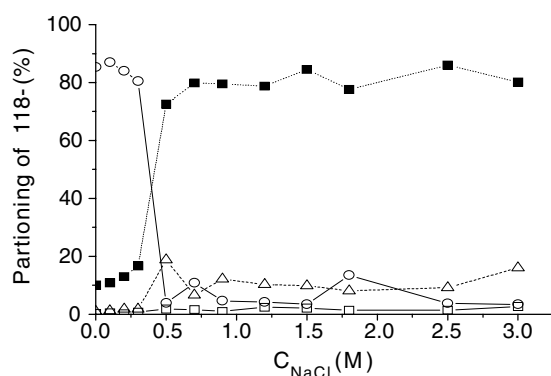
Fig. 1. Partitioning of 118− as a function of NaCl concentration: aqueous phase (○); phenolic phase (△); adsorption on the walls of the tube (□); water-phenol interface (■).

of NaCl concentration. Below 0.3 M NaCl the ssDNA remains in the aqueous phase; it is almost completely removed from this phase at higher salt concentrations. Only a small amount of ssDNA is transferred to the organic phase (typically 10% or less of the radioactive material) or is found adsorbed on the walls of the tubes (typically 6% or less of the radioactive material). The amount of radioactivity found in these three phases (aqueous phase, organic phase and surface of the tube) represents only 20% of the total radioactivity above 0.5 M NaCl. Conversely, the difference between the total radioactivity and this amount (represented by full squares in Fig. 1) accounts for 80% of the total radioactivity. To localize this missing radioactivity, we performed a similar partitioning experiment at 0.85 M NaCl in a bigger (15 ml) tube also treated with dimethyldichlorosilane beforehand, and obtained an overnight autoradiography of the tube (an experiment suggested to us by Gilbert Zalczer). Figure 2 shows a picture of the tube, and the autoradiography of a portion of it. There is a peak located at the water-phenol interface (Fig. 2, bottom), which accounts for the missing radioactivity (there is no radioactivity at the air-water interface). We conclude that above 0.5 M NaCl the missing radioactivity is located at the water-phenol interface.

The experiments described below in the water-phenol system have been performed at 0.85 M NaCl. We therefore characterized in greater detail the partitioning of ssDNA at this concentration by repeating this experiment 10 times: 1) $80 \pm 8\%$ of the ssDNA is adsorbed the water-phenol interface; 2) $6 \pm 1\%$ of the ssDNA is transferred in the phenolic phase; 3) 3–5% the ssDNA is adsorbed on the walls of the tubes; 4) 3–5% of the total radioactivity is present in the aqueous phase. This radioactivity does not correspond to ssDNA but to γ ^{32}P-ATP (aliquots of the aqueous phase run on a polyacrylamide gel never show the ssDNA band but only the γ ^{32}P-ATP band; data not shown). We also obtained similar results in experiments with the complementary ssDNA 118+ (data not shown).

The reversibility of the adsorption as a function of NaCl concentration was determined in the following manner. We first adsorbed the ^{32}P-labeled 118+ by vortexing and centrifugation as described above in the presence of
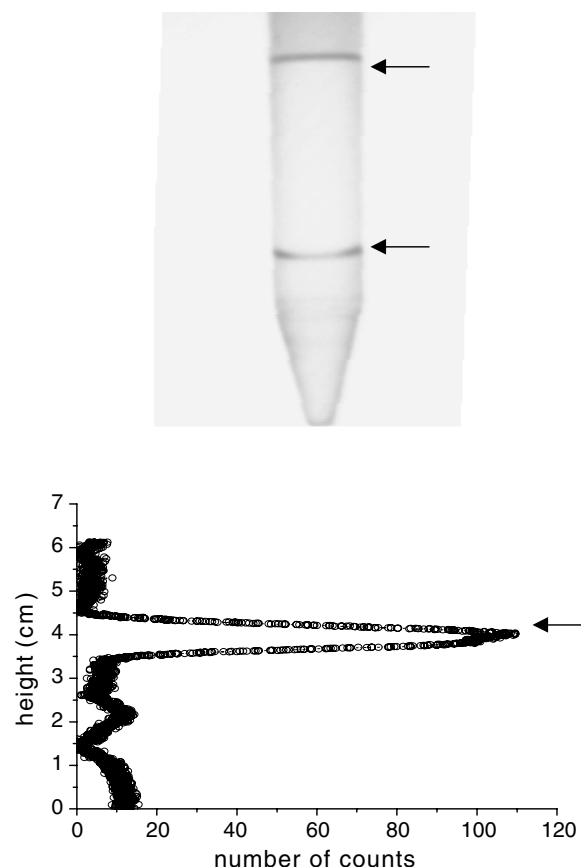

Fig. 2. Top: picture of a 15 ml silanized tube containing a mixture of brine (0.85 M NaCl in TE buffer solution) and phenol (40% in volume) plus 0.125 nM ^{32}P-labeled 118−. Top arrow: air-water interface; bottom arrow: water-phenol interface. Distance between the two arrows: 6 cm. Bottom: autoradiography of a portion of the tube, showing a peak at the water-phenol interface (arrow).

different NaCl concentration between 0 and 1 M NaCl. We measured the amount of radioactivity present in the aqueous phase (Fig. 3, open circles). We then prepare 10 different tubes where the ^{32}P-labeled 118+ was adsorbed in the presence of 1 M NaCl. We removed 155 μl of the aqueous phase, and replace it by 155 μl of a phenol-saturated TE solution containing different NaCl concentrations. We again vortexed and centrifuged the tubes and determined the amount of radioactivity present in the aqueous phase. Figure 3 (full squares) shows the result of this desorption experiment. The adsorbed 118+ is fully desorbed at low salt (0.1 M and below). One observes a hysteresis between 0.2 and 0.6 M NaCl. The differential partitioning of the ions between the two phases could account for this hysteresis. No desorption is observed at high salt concentration (above 0.6 M). We have further checked this lack of desorption at high salt concentration in two ways: first by incubating for 12 hours the two-phase system prior to the vortexing/centrifugation steps, and second by repeating several times the desorption experiment. In both cases we observed no release of the adsorbed DNA. The adsorption is therefore irreversible at high salt under the

Table 1. Partitioning of 118− for 14 organic solvents. The salt concentration at the onset of the adsorption was determined, as well as the percentage of 118− remaining in the aqueous phase at 3 M NaCl (except for fluorobenzene, where it was determined at 2.5 M NaCl). The organic compounds are sorted by increasing efficiency in each sub-group.

| Category	Compound	Critical salt concentration for ssDNA adsorption	ssDNA in aqueous phase at 3 M NaCl (%)
HYDROPHOBIC	Dodecane	–	100
	Carbon tetrachloride	–	100
	Dichloromethan	2.5	51
	Chloroform	2.5	33
AROMATIC	Toluene	–	100
	Aniline	–	100
	Bromobenzene	1.4	41
	Iodobenzene	1.4	54
	Chlorobenzene	1	57
	Fluorobenzene	0.3	22 (2.5 M)
	Guaiacol	0.5	10
	Phenol	0.3	0
PRIMARY ALCOHOL	Butanol	–	100
	Benzylalcohol	2	48
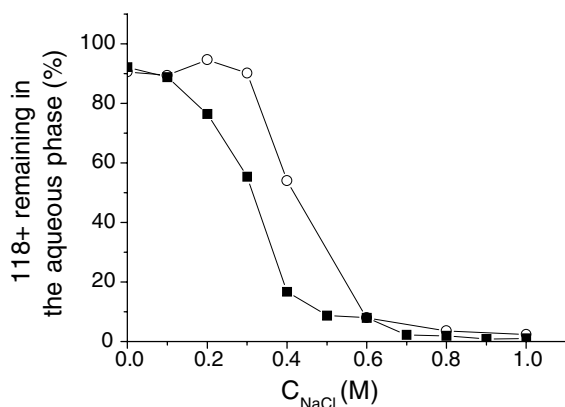
Fig. 3. Reversibility of the adsorption of 118+ as a function of NaCl concentration. Percentage of 118+ in the aqueous phase: adsorption (○); desorption (■).

Fig. 4. Percentage of 118− remaining in the aqueous phase as a function of salt concentration for three solvents: phenol (○), guaiacol (□) and fluorobenzene (△).

experimental conditions later used in this work. We will refer to this adsorption as a strong or an irreversible adsorption.

3.2 Partitioning of ssDNA using other organic solvents

We performed similar partitioning experiments using 13 other organic solvents that are only partially miscible with water. The results are summarized in Table 1. The solvents are divided into three classes: simple hydrophobic solvents, aromatic solvents and primary alcohols. Five solvents are unable to remove the ssDNA from the aqueous phase, even at 3 M NaCl (dodecane, toluene, carbon tetrachloride, butanol and aniline). Dichloromethane and chloroform begin to adsorb ssDNA above 2.5 M NaCl only. The other solvents are all planar aromatic compounds. The best solvents are fluorobenzene, guaiacol and phenol.
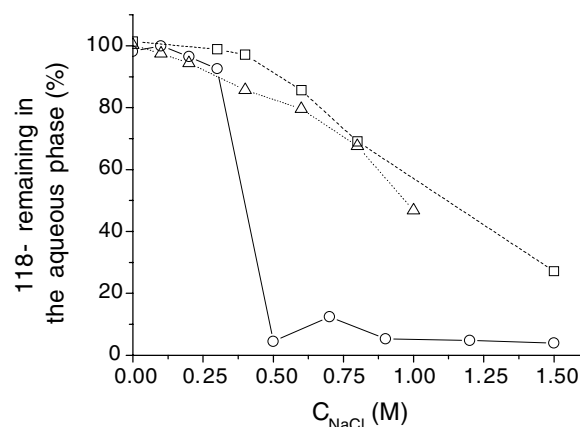
Figure 4 shows that they all start to remove the ssDNA from the aqueous phase at low NaCl concentrations (above 0.3 M NaCl for fluorobenzene and phenol, and 0.5 for guaiacol). However, phenol is the most efficient solvent, allowing a complete adsorption above 0.5 M, a salt concentration where about 80% of the ssDNA is still in the aqueous phase in the presence of fluorobenzene or guaiacol.

3.3 Renaturation and transfer to the aqueous phase of an adsorbed ssDNA in the presence of its complementary strand

As shown before, at 0.85 M NaCl, 80% of the ssDNA (118+ or 118−) is irreversibly adsorbed at the water-phenol interface. We performed the following experiment at this salt concentration. We first adsorbed the
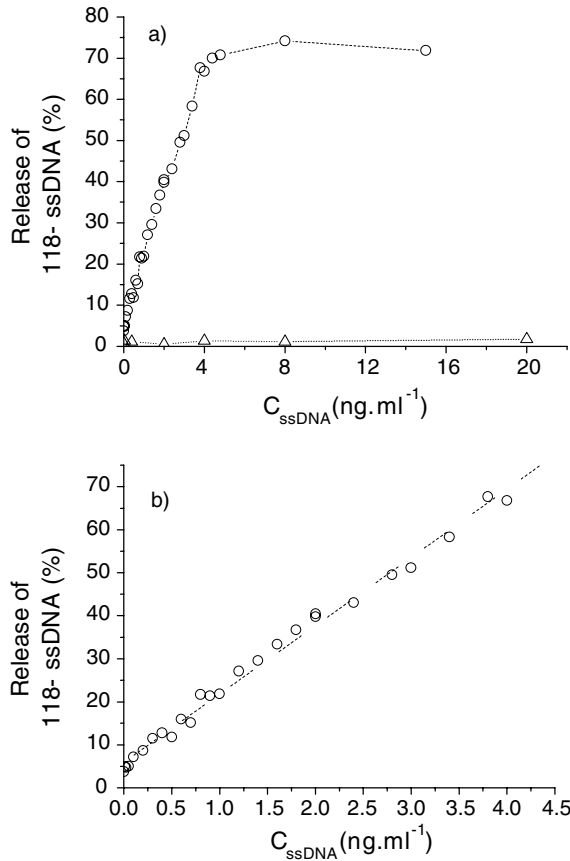
Fig. 5. a) Release of adsorbed 118− by the complementary polynucleotide 118+. Percentage of released 118− as a function of added 118+ (○). Control experiment: percentage of released 118− as a function of added 118− (△). b) Initial percentage of released 118− as a function of added 118+: experimental data (○), linear fit (dashed line).

^{32}P-labeled 118− by vortexing and centrifugation as described above, and then removed 155 μl of the aqueous phase. We replaced it by 155 μl of a TE solution containing the same concentrations of phenol and NaCl, and various amounts of the unlabeled complementary strand 118+. We again vortexed and centrifuged the tube, and then determined the amount of radioactivity present in the aqueous phase. Figure 5a shows that the addition of increasing amounts of the complementary strand 118+ leads to the progressive release of the adsorbed 118− in the aqueous phase. Up to $70 \pm 10\%$ of the 118− can be released; this plateau value is obtained when a concentration of 4 ng/ml of 118+ is reached, corresponding to the amount of 118− present in the tube. The release therefore involves the formation of a 1-1 complex. The release is specific to the complementary strand, since it is not observed when similar amounts of the same strand 118− (instead of the complementary strand) are added in the aqueous phase (Fig. 5a, open triangles). We analyzed the released material by gel electrophoresis: it consists solely of a renatured double-stranded DNA (data not shown). Since the adsorption at the water-phenol interface is irreversible for each of the two complementary ssDNA taken separately

in our experimental conditions, the renaturation reaction must have been initiated at the interface. Furthermore, the double-stranded DNA that is the outcome of this reaction is not adsorbed at the interface (it partitions entirely in the aqueous phase in our experimental conditions). Thus, as soon as a double-stranded DNA segment is nucleated, it is expelled from the interfacial region. Figure 5b further shows that there is initially a strict linear relation between the amount of added 118+ and the amount of released 118−, which confirms that the release involves a stoichiometric process. The slope of the curve in Figure 5b is equal to 0.63 ± 0.01. This value corresponds to the product of the two fractions of adsorbed ssDNA ($0.8 \times 0.8 = 0.64$). This confirms the strict interfacial nature of the reaction: only the adsorbed chains can participate in the reaction. The height of the plateau ($70 \pm 10\%$) corresponds to the complete release of 118− by the renaturation reaction.

3.4 Effects of vortexing on adsorption and renaturation

3.4.1 Adsorption without vortexing

Figure 6a shows the percentage of radioactive material removed from the aqueous phase as a function of time in the absence of vortexing. According to Figure 6b, this percentage increases at first linearly with the square root of time, up to about 1.5×10^4 s. This dependency is suggestive of an irreversible, diffusion-controlled process [67–69]. We will model the kinetic of ssDNA adsorption assuming that the adsorption is diffusion limited. At time $t = 0$ the bulk number of ssDNA chains is N_0 ($N_0 = C_0 \times V$). The chain concentration C_0 is supposed to remain constant close to the air-water interface. This assumption, known as a semi-infinite approximation, will be justified *a posteriori*. The number $N(t)$ of ssDNA chains adsorbed at time t at the water-phenol interface is obtained by solving a one-dimensional diffusion equation with boundary conditions pertaining to the conical geometry of our system (Fig. 6c). Under these conditions the rate of adsorption is given by

$$\left.\frac{\mathrm{d}N\left(t,z\right)}{\mathrm{d}t}\right|_{z=0} = \Omega C_0 \sqrt{D_{3\mathrm{d}}}\frac{1}{\sqrt{t}} \qquad (1)$$

with $\Omega = 4\sqrt{\pi}\sin\left(\frac{\pi}{12}\right)\left(ah + \frac{h^2}{3}\right)$. In this equation, $D_{3\mathrm{d}}$ is the three-dimensional diffusion coefficient of the ssDNA chain 118−, h is the height of the water column, a is the distance between the water-phenol interface and the apex of the cone, and the interface lies at $z = 0$ (see Fig. 6c). By integrating both sides of this equation and using the boundary condition $N(t = 0) = 0$, we obtain the following expression for the number of adsorbed ssDNA chains as a function of time:

$$N(t) = 2\Omega C_0 \sqrt{D_{3\mathrm{d}}}\sqrt{t}\,. \qquad (2)$$

In our experiments, 5% of the total amount of radioactivity corresponds to $\gamma\,^{32}$P-ATP, which always remains in the aqueous phase. In order to model the experimental

Fig. 7. Adsorption with vortexing of 118− (0.125 nM) at the brine (0.85 M NaCl in TE)-phenol (40% in volume) interface as a function of time of vortexing for various vortexing velocities (in rounds per minute).

Equation (3) has been used to fit the first regime of adsorption (Fig. 6a). The values of the fitting parameters are:

Parameters	D_{3d} (cm^2 s^{-1})	A
Values	$2.4 \times 10^{-7} \pm 9.6 \times 10^{-9}$	$4.6 \times 10^{-2} \pm 8.2 \times 10^{-3}$

The value of the constant A is in good agreement with the value of 5% determined above. From the value obtained for D_{3d} we can estimate the characteristic time t_h required to explore the height h of the aqueous phase using the relation $h^2 \approx 6 D_{3d} t_h$. We obtain a time t_h of about 4.4×10^5 s. The time t_h corresponds to time required to deplete the air-water interface. Since the fitted experimental data have been obtained on a much shorter time scale, the semi-infinite approximation is indeed valid.

3.4.2 Adsorption with vortexing

The effects of the duration of vortexing and of the vortexing velocity on the kinetics of adsorption of the ^{32}P-labeled ssDNA 118− are shown in Figure 7. At the highest vortexing velocity (2400 rpm), a complete adsorption is achieved immediately (that is within the first five seconds). The rate of adsorption increases with the vortexing velocity for lower velocities. The curves suggest the existence of two regimes. At first there is a roughly linear increase of the amount of adsorbed DNA with time. In the second regime the increase is much reduced; the amount of adsorbed ssDNA at this quasi-plateau increases with vortexing velocity.

3.4.3 Renaturation without vortexing

Figure 8a shows the percentage of renatured DNA as a function of time obtained in the two-phase system in the
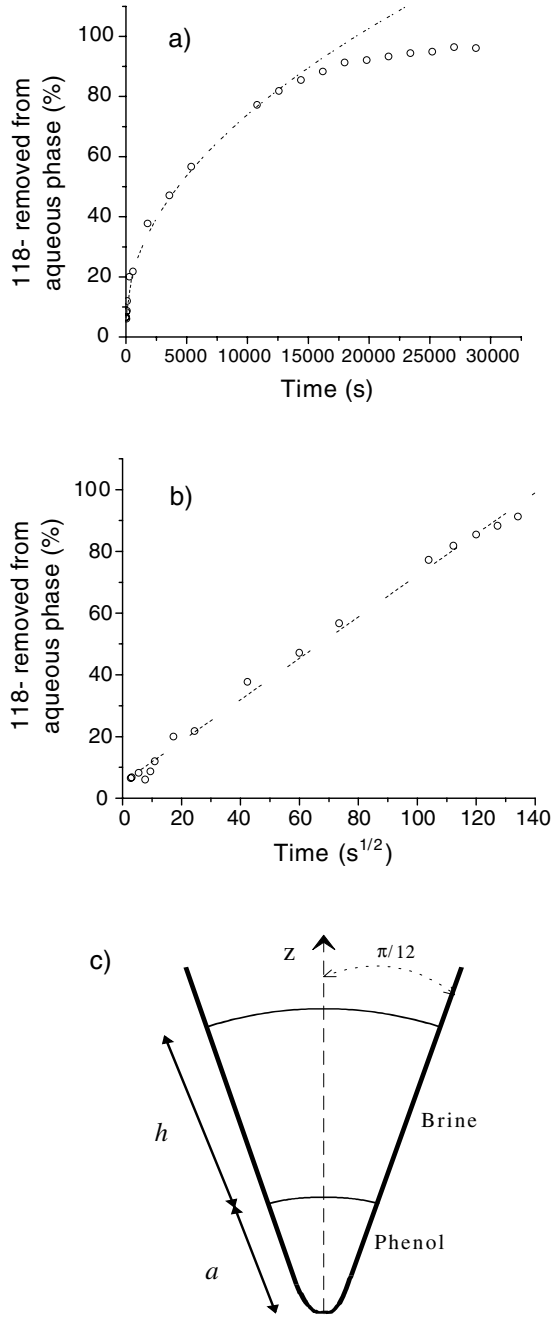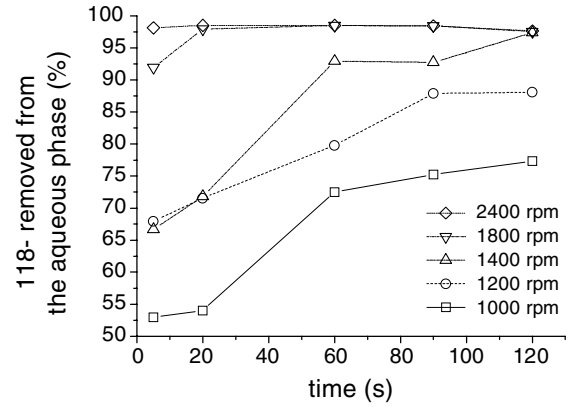

Fig. 6. a) Percentage of 118− (0.125 nM) removed from the aqueous phase in the absence of shaking in a biphasic mixture of brine (0.85 M NaCl in TE) and phenol (40% in volume) as a function of time. Experimental data (◯). The dashed line is the fit obtained with equation (3). b) Initial percentage plotted as a function of the square root of time. c) Schematic drawing of the experimental tube, $a = 0.5$ cm and $h = 0.8$ cm.

results, a constant A should therefore be added to the right-hand side of equation (2).

$$\frac{N(t)}{N_0} = \frac{2\Omega\sqrt{D_{3d}}}{V}\sqrt{t} + A. \qquad (3)$$
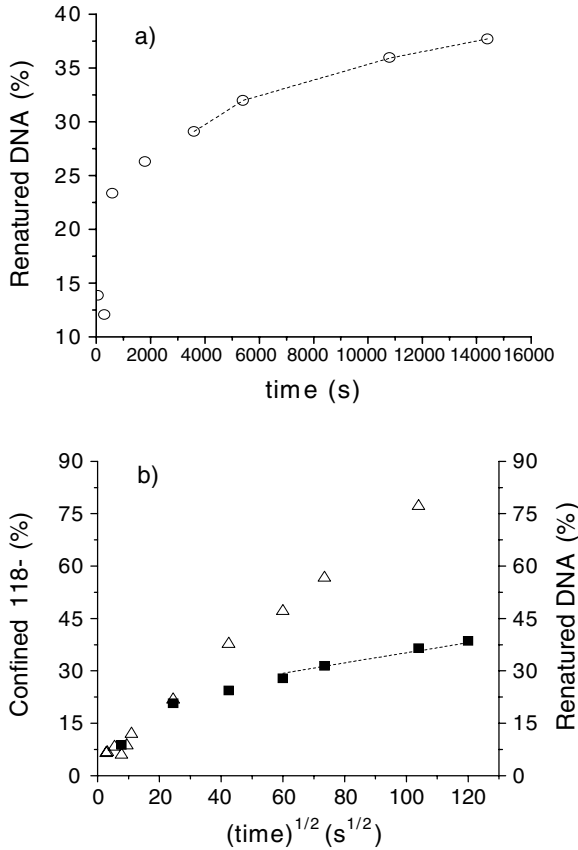
Fig. 8. a) DNA renaturation without vortexing of the two complementary polynucleotides 118+ and 118− (0.125 nM each) at the brine (0.85 M NaCl in TE)-phenol (40% in volume) interface as a function of time. Experimental data (○). The dashed line is the fit obtained with equation (13). b) Comparison of the rate of DNA renaturation without vortexing (data of Fig. 8a) (■) and of the rate of adsorption of 118− at the brine-phenol interface (data from Fig. 6b) (△) as a function of the square root of time. The curve describing the rate of renaturation (■) has been translated along the ordinate axis in order to be superimposed with the adsorption at short times.

absence of vortexing (during the renaturation stage). In this experiment, ^{32}P-labeled ssDNA 118− (125 pM in the aqueous phase) was first adsorbed at the water-phenol interface by vortexing and centrifugation. We then removed 155 μl of the aqueous phase, and replaced it by 155 μl of a TE solution containing the same concentrations of phenol and NaCl, and the ^{32}P-labeled complementary strand 118+ (also at 125 pM). The two-phase system was left to react without agitation. The reaction was quenched by the addition of enough TE buffer (600 μl TE buffer) to destroy the two-phase system, and an aliquot was analyzed by gel electrophoresis. The rate renaturation is slow, less than 40% of the DNA having renatured within three hours. A comparison of the rate of this reaction with the rate of adsorption observed without agitation (Fig. 8b) shows that initially the two processes occur at similar rates; later on, renaturation becomes the slower of the two processes. This is fully consistent with the conclusion drawn above that renaturation takes place at the interface: the complementary

strand must first be adsorbed before it renature. Later on the percentage of renatured DNA increases linearly with the square root of time (Fig. 8b). We now propose a model to explain this dependency.

The renaturation reaction has two kinetic components: the ssDNA must be adsorbed and then it has to search the interface for its complementary strand to renature. At the beginning of the reaction, adsorption and renaturation occur at similar rates. Renaturation is therefore not rate limiting: the concentration of adsorbed 118− is high enough, and when the 118+ reaches the interface it encounters quickly its complementary and forms a dsDNA which is expelled into the aqueous phase. As the reaction proceeds, the concentration of available adsorbed 118− decreases and therefore the rate of the bimolecular reaction between the two complementary strands slows down. In this second regime the rate of the reaction depends on a combination of the diffusion-controlled rate of adsorption and the interfacial recombination. According to this picture, at still longer times, there is a third regime where the rate of reaction is given solely by the rate of recombination at the interface (we do not reach this regime in the present study). The transition between the first and the second regime can be described using the standard terminology of surface chemistry [70,71]. When a reaction between two compounds is catalyzed by a surface, it is possible to distinguish two types of processes. In the first process, the reaction occurs between the two adsorbed compounds, and involves a surface diffusion of at least one of them. This is known as a Langmuir-Hinshelwood mechanism. In the second process, there is no need for a surface diffusion: the reaction occurs between the adsorbed compound and the second compound coming from the volume above the surface. The encounter between the two compounds involves only a 3-dimensional diffusion. This is known as an Eley-Rideal mechanism. In our case, the first regime is compatible with an Eley-Rideal mechanism where 118+ encounters the adsorbed 118− through a 3-dimensional diffusion (Fig. 9, path A). A surface diffusion step (Fig. 9, path B) may be present, but too fast to be detected. In the second regime, the rate of renaturation becomes slower than the rate of adsorption. This corresponds to a Langmuir-Hinshelwood mechanism (path B in Fig. 9).

We will model the recombination reaction at the interface assuming a diffusion-controlled annealing process. We further assume that the 118− and the 118+ ssDNA have the same shape and the same two-dimensional diffusion coefficient D_{2d}. Let us call the 118− the target and the 118+ the probe. We describe the target molecule as a disc of radius R_1 corresponding to half the end-to-end distance of the 118− chain. A given time t, $N_{target}(t)$ target molecules are embedded in the water-phenol interface, and the average area per target molecule can be estimated assuming that the distribution of target molecules on the interface of area S is homogeneous. The average area per target molecule is equal to:

$$A_{target}(t) = \frac{S}{N_{target}(t)} = \pi \left[R_2(t)\right]^2 , \qquad (4)$$
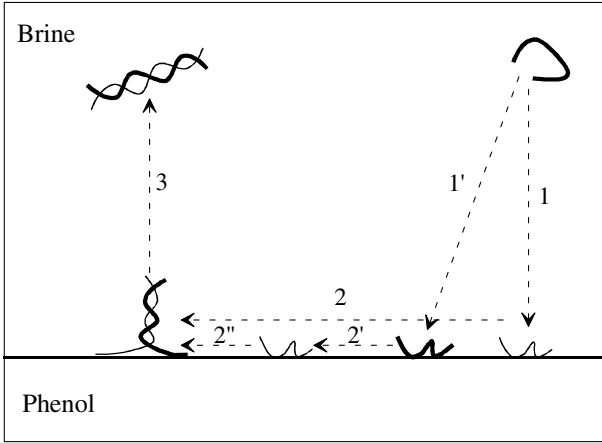
Fig. 9. The two kinetics paths A and B of the renaturation reaction at water-phenol interface in the absence of vortexing. A: 1) The probe molecule (thick line) encounters directly the target molecule (thin line) through a 3-dimensional diffusion; 2) the dsDNA is formed; 3) the dsDNA form is expelled from the interface to the aqueous phase. B: 1′) The probe molecule is first adsorbed at the interface through a 3-dimensional diffusion; 2′) the probe molecule and the target molecule encounter each other at the interface through a 2-dimensional diffusion; 2″) the dsDNA is formed; 3) the dsDNA form is expelled from the interface to the aqueous phase.

where $R_2(t)$ is a radius. The problem of the capture of a probe molecule by a target molecule corresponds therefore to a diffusion in a hollow cylinder of inner radius R_1 and outer radius R_2. Diffusion in a hollow cylinder has attracted considerable attention over time, and several solutions corresponding each to a particular boundary initial value have been proposed [68,72–74]. To our knowledge, these solutions deal only with situations where the radii R_1 and R_2 are independent of time. In these cases, the diffusion equation in cylindrical coordinates can be solved following the method of separation of space and time variables [68]. In the present situation, when a probe encounters a target molecule, the formed product is expelled from the interface into the bulk. Therefore, this reaction is an interfacial annihilation reaction. As the reaction between the target and probe molecules proceeds, the water-phenol interface is depleted from target molecules and therefore the average area per target molecule increases. The present problem is that of the diffusion in a hollow cylinder with a moving boundary $R_2(t)$. Under these circumstances it is not possible to solve the diffusion equation by separating time and space variables. To overcome this mathematical problem, we use a steady-state approximation expected to be valid at long times, when the concentration of target molecules becomes low enough. Under this assumption, the rate of capture of a probe molecule by a target molecule is such that the flux of probe molecules injected at r (the in-plane polar coordinate) equals the flux k_{capture} of probe molecules which disappear at $2R_1$:

$$k_{\text{capture}} = 8\pi R_1 D_{2\text{d}} \left. \frac{\mathrm{d}P}{\mathrm{d}r} \right|_{r=2R_1}, \qquad (5)$$

where $P(r)$ is the probability to find a probe molecule at position r (in-plane polar coordinate) away from a target molecule. In a cylindrical symmetry the diffusion equation under steady-state condition is written as

$$\frac{\mathrm{d}}{\mathrm{d}r}\left(r \frac{\mathrm{d}P(r)}{\mathrm{d}r} \right) = 0, \qquad 2R_1 < r < R_2 \qquad (6)$$

with boundary conditions $P(2R_1) = 0$, $P(R_2) = 1$. Such conditions imply that 1) the target surface concentration is very dilute and 2) that there is a reservoir of probe molecules.

Berg and Purcell [75] studied a similar problem for a plane with fixed boundary conditions. They concluded that the two-dimensional capture rate will dominate solely if the two-dimensional rate of capture is much bigger than the three-dimensional rate. In our case the situation is somewhat different. Using the same approach as Berg and Purcell, we assume that the steady-state rate at the surface is reached when the rate of capture k_{capture} at two dimensions is equal to the rate of adsorption at three dimensions. Using this assumption and the fact that the variation of the number of probe molecules $N_{\text{probe}}(z,t)$ in the z (vertical) direction is independent of the in-plane variations of the number $N_{\text{probe}}(r,t)$ of probe molecules, we can write an additional boundary condition to equation (6):

$$\mathrm{d}N_{\text{probe}}(r,z)|_{z=0} = N_{\text{probe}}(r) \left. \frac{\mathrm{d}N_{\text{probe}}(z)}{\mathrm{d}z} \right|_{z=0} \mathrm{d}z$$
$$+ N_{\text{probe}}(z=0) \frac{\mathrm{d}N_{\text{probe}}(r)}{\mathrm{d}r} \mathrm{d}r = 0.$$

Using the above considerations, the number of probes $N(r)$ for $2R_1 < r < R_2$ is therefore given by

$$N_{\text{probe}}(r,t) = \left(\left. \frac{\mathrm{d}N_{\text{probe}}(t,z)}{\mathrm{d}z} \right|_{z=0} \right) \frac{\ln\left(\frac{r}{2R_1}\right)}{\ln\left(\frac{R_2}{2R_1}\right)}, \qquad (7)$$

where the first term in the bracket in the right-hand side corresponds to the gradient of concentration of probes molecule in the direction normal to the interface. As the probability $P(r) = N_{\text{probe}}(r,t)/N_{\text{probe}}(r,t=0)$, the rate of capture is equal to

$$k_{\text{capture}} = \frac{\Omega}{V} \frac{8\pi}{\ln\left(\frac{R_2}{2R_1}\right)} \frac{D_{2\text{d}}}{\sqrt{D_{3\text{d}}}} \frac{1}{\sqrt{t}}. \qquad (8)$$

The rate of capture depends on time and on the number of target molecules. Two extreme cases can be considered. 1) If $R_2 = 2R_1$ the value of the capture rate diverges and goes to infinity. This condition corresponds to the close packing of target molecules at the interface. This situation corresponds to a very concentrated interface and is beyond the range of validity of the calculated rate of capture. However, the divergence of the two-dimensional capture rate indicates that for a concentrated interface the two-dimensional diffusion process is not the rate limiting

step. 2) If R_2 is sufficiently larger than R_1, the situation corresponds to a dilute interface, where the steady-state approximation can be applied. Under this condition the two-dimensional rate of capture contributes to the overall rate of the reaction.

The variation of number of target molecule at the interface is equal to

$$\frac{\mathrm{d}N_{\mathrm{target}}(t)}{\mathrm{d}t} = -k_{\mathrm{capture}}(t, N_{\mathrm{target}}(t)) N_{\mathrm{target}}(0) , \quad (9)$$

where $N_{\mathrm{target}}(0)$ is the initial number of target molecules at the interface. Combining equations (8) and (9), we obtain after integration

$$\left[2\ln\left(\frac{R_s}{2R_1}\right) - \ln(N_{\mathrm{target}}(t)) + 1 \right] \frac{N_{\mathrm{target}}(t)}{2}$$
$$- \left[2\ln\left(\frac{R_s}{2R_1}\right) - \ln(N_{\mathrm{target}}(0)) + 1 \right] \frac{N_{\mathrm{target}}(0)}{2} =$$
$$- N_{\mathrm{target}}(0) 16\pi \frac{\Omega}{V} \frac{D_{2\mathrm{d}}}{\sqrt{D_{3\mathrm{d}}}} \sqrt{t} , \quad (10)$$

where $R_s = \sqrt{\frac{S}{\pi}}$ is the radius of the interface; note that this relation between R_s and S is based on the assumption that the interface is plane. Under the close-packing condition the number of target molecules lying on the interface is equal to the square of the ratio of the radius of the interface and the radius of the target: $N_{\mathrm{close\ packing}} = \left(\frac{R_s}{R_1}\right)^2$. Under the hypothesis that the concentration of target molecule is very dilute at the interface ($N_{\mathrm{target}}(t) \ll N_{\mathrm{close\ packing}}$ at any time) equation (10) can be approximated to

$$N_{\mathrm{target}}(t) \approx -\frac{32\pi N_{\mathrm{target}}(0) \Omega}{\left[2\ln\left(\frac{R_s}{2R_1}\right) + 1 \right]} \frac{D_{2\mathrm{d}}}{\sqrt{D_{3\mathrm{d}}}} \frac{\sqrt{t}}{V} + N_{\mathrm{target}}(0) . \quad (11)$$

As pointed out above the recombination reaction at the interface can be considered as an annihilation reaction. Therefore, the fraction of renatured ssDNA is equal to

$$\theta_{\mathrm{dsDNA}}(t) = \frac{N_{\mathrm{target}}(0) - N_{\mathrm{target}}(t)}{N_{\mathrm{target}}(0)} =$$
$$\frac{32\pi}{\left[2\ln\left(\frac{R_s}{2R_1}\right) + 1 \right]} \frac{\Omega}{V} \frac{D_{2\mathrm{d}}}{\sqrt{D_{3\mathrm{d}}}} \sqrt{t} \quad (12)$$

and the fraction of renatured ssDNA should change as the square root of time.

As explained above the considered reaction has two kinetics components, the first one is the three-dimensional adsorption process and the second one is the two-dimensional process. These two processes correspond to the two asymptotic limits of the reaction (respectively at short and long times). In the intermediate regime the two kinetic components work cooperatively to form the dsDNA molecule. To model the data presented in Figure 8b, equation (12) should be modified. The two-dimensional

steady state can be considered to have been reached after a time t_0, where the $\theta_{\mathrm{dsDNA}}(t_0)$ fraction of dsDNA has already been formed. Under these conditions equation (12) should be modified, replacing t by $t - t_0$ and adding a constant equal to $\theta_{\mathrm{dsDNA}}(t_0)$:

$$\theta_{\mathrm{dsDNA}}(t) = \frac{32\pi}{\left[2\ln\left(\frac{R_s}{2R_1}\right) + 1 \right]} \frac{\Omega}{V} \frac{D_{2\mathrm{d}}}{\sqrt{D_{3\mathrm{d}}}} \sqrt{(t - t_0)}$$
$$+ \theta_{\mathrm{dsDNA}}(t_0) . \quad (13)$$

Equation (13) has been used to fit the last part of the experimental data presented in Figure 8b. The value of R_s was determined using a vernier: $R_s = 0.13$ cm ($\pm 5\%$). The values of the fitted parameters are presented below:

Parameters	$\frac{D_{2\mathrm{d}}}{\left[2\ln\left(\frac{R_s}{2R_1}\right)+1\right]}$ $(\mathrm{cm}^2\,\mathrm{s}^{-1})$	t_0 (s)	$\theta_{\mathrm{dsDNA}}(t_0)$
Values	1.7×10^{-10} $\pm 3.5 \times 10^{-12}$	3390 ± 60	$0.28 \pm 2 \times 10^{-3}$

One can obtain lower and upper estimates for R_1 as follows. The end-to-end distance R_1 of the target molecule is given by: $R_1 \approx \frac{1}{2} b N^\nu$, where ν is the Flory exponent ($1/2 \leqslant \nu \leqslant 1$ in two dimensions) and b is the size of a monomer. Possible values of b range typically between $b = 3.4$ Å (obtained when bases are stacked as in a DNA double helix) and $b = 7$ Å (corresponding to a fully stretched phosphate backbone). One can therefore obtain lower (for $\nu = 1/2$ and $b = 3.4$ Å) and upper (for $\nu = 1$ and $b = 7\times$ Å) estimates for R_1: 19 Å $\leqslant R_1 \leqslant 413$ Å, and from these bracket the two-dimensional diffusion coefficient: $3.4 \times 10^{-9} \pm 7.1 \times 10^{-11}\,\mathrm{cm}^2\,\mathrm{s}^{-1} \leqslant D_{2\mathrm{d}} \leqslant 4.4 \times 10^{-9} \pm 9.3 \times 10^{-11}\,\mathrm{cm}^2\,\mathrm{s}^{-1}$.

The two-dimensional diffusion coefficient depends weakly (logarithmically) on the conformation of the ssDNA chains, leading to a narrow range of possible values for $D_{2\mathrm{d}}$: $D_{2\mathrm{d}} = 3.9 \times 10^{-9} \pm 6 \times 10^{-10}\,\mathrm{cm}^2\,\mathrm{s}^{-1}$.

3.4.4 Renaturation with vortexing: PERT

Figure 10a shows the kinetics of renaturation of the two complementary ssDNA 118+ and 118− (1.66 pM each) in a 100 μl mixture containing 90 μl of TE plus 0.85 M NaCl and 10 μl phenol vigorously shaken (2400 rpm). This corresponds precisely to the experimental conditions of PERT [1] (vigorous shaking of denatured DNA, equal amounts of complementary strands). The mixture was vortexed at 2400 rpm for various times, the reaction was quenched by the addition of enough TE buffer (100 μl TE buffer) to destroy the emulsion, and an aliquot was analyzed by gel electrophoresis. The reaction is quite fast: about two thirds of the DNA have renatured within 30 s. Nevertheless, by comparing the rates of adsorption and of renaturation (Fig. 7 and Fig. 10a), we see again that
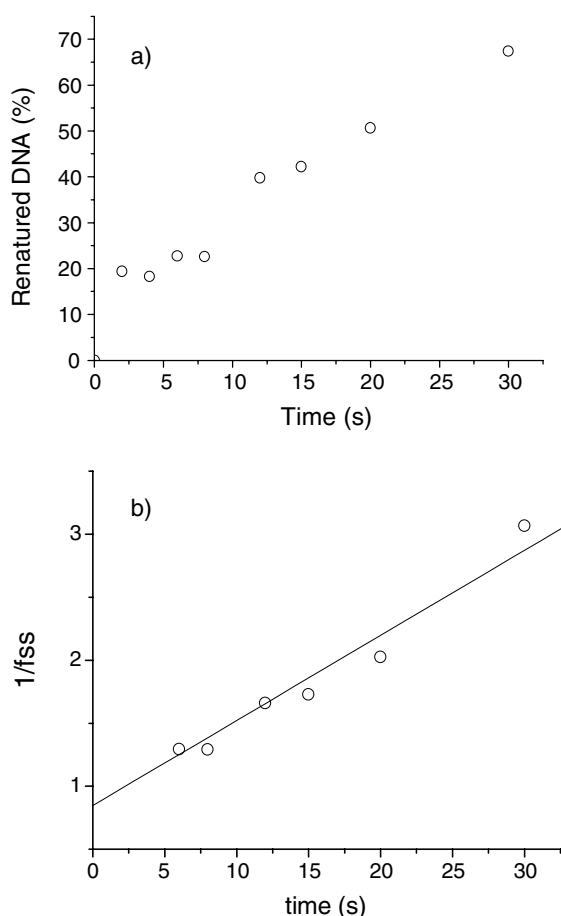
Fig. 10. DNA renaturation by vortexing of the two complementary polynucleotides 118+ and 118− (0.125 nM each) at the brine (0.85 M NaCl in TE)-phenol (40% in volume) interface. a) Percentage of renatured DNA as a function of time. b) Time variation of the inverse of the survival probability (1/fss) showing the experimental data (○) and the linear fit.

become negligible. It is replaced by a convective flow that controls the arrival and the removal of material at the interface between water and phenol droplets. We calculated the rate of the reaction assuming a classical bimolecular process. The validity of this calculation can be questioned. The system is not under a steady-state flow and the distribution of the reactants is not uniform in the solution. These inhomogeneities could lead to a hydrodynamic instability and in turn radically change the kinetics of the reaction [76].

4 Discussion

We have studied an interfacial DNA renaturation, taking place at a water-phenol interface. We have used a decoupling scheme to establish the interfacial nature of this reaction. The decoupling scheme has led to a characterization of a salt-dependent interfacial confinement of single-stranded DNA, which was studied with and without shaking. We have tested 13 other organic solvents for their capacity of adsorbing ssDNA at the water-organic solvent interface at room temperature in the presence of NaCl. Phenol is the most efficient of all tested solvents. The study of DNA renaturation in the absence of shaking shows the existence of a regime where the rate of the reaction depends on the two-dimensional diffusion of the complementary single-strands. We have determined both the three-dimensional and two-dimensional diffusion coefficients of the ssDNA. The two-dimensional coefficient D_{2d} is about 60 times smaller than the three-dimensional coefficient D_{3d}. We have also investigated the effect of shaking on the interfacial renaturation. We established the interfacial nature of PERT in extremely dilute DNA solutions and measured the bimolecular rate constant for the reaction in these conditions. We will now discuss these results following the plan outlined in the introduction.

4.1 Adsorption and renaturation of DNA in the water-phenol two-phase system

4.1.1 Water-phenol mixtures; salt effects on such mixtures

We study the behavior of nucleic acids in a water-phenol two-phase system, at various salt concentrations. The discussion of our data requires some knowledge of water-phenol mixtures with and without added salt. Mixtures of water and phenol have been avidly studied over the last century and a wealth of experimental data is available both for bulk (see [77,78] and further references therein, [79]) and interfacial properties (although only at the air-solution interface (see [80,81] and further references therein). At room temperature water and phenol are only partially miscible (9% phenol in water and 29% water in phenol in weight percent) [79]. The two solvents become miscible above 66 °C (in other words the system has an upper critical solution temperature). The phase diagram has a complicated structure at low temperature (below 10 °C) [78,82]: it is closed by the formation of a

renaturation is the slower of the two processes. We know from the experiment on the rate of adsorption at this vortexing velocity that each complementary ssDNA is completely adsorbed within five seconds. In the renaturation experiment, all the data obtained after 5 seconds therefore involve complementary strands that have been previously completely adsorbed. The renaturation process between 5 and 30 s takes place exclusively at the water-phenol interface. This establishes the interfacial nature of PERT in this experiment. Assuming that the reaction follows a standard bimolecular kinetics, the reciprocal of f_{ss}, the fraction of DNA remaining single-stranded at time t is expected to grow linearly with t according to: $1/f_{ss} = k_2 C_0 t + 1$, where k_2 is the bimolecular rate constant, and C_0 the molar concentration of single-strands (here $C_0 = 1.66$ pM). The reciprocal of f_{ss} has been plotted as a function of time in Fig. 10b. The rate constant obtained by a linear fit yields $k_2 = 4.2 \pm 0.4 \times 10^{10}$ M^{-1}s^{-1}. This fit is only valid for times $t > 5$ s. The exact meaning of this rate constant is complex: the solution is vigorously vortexed, and the three-dimensional diffusion process has

phenol hydrate (with formula $(C_6H_5OH)_2H_2O$). The crystal structure of phenol hydrate has been determined [83]. Phenol and water molecules are connected by hydrogen bonds, each water molecule being surrounded by four phenol molecules with a distorted tetrahedral structure.

Both adsorption and interfacial renaturation requires the presence of monovalent salts (typically in the order of one mole per liter for PERT [1]). The addition of salt modifies both bulk and interfacial properties of water-phenol mixture. Indeed, the addition of salt greatly enlarges the two-phase region in the temperature *versus* concentration water-phenol phase diagram [77,84–88]. The miscibility of the two solvents is decreased at fixed temperature, and the upper critical solution temperature is increased. The mutual solubility of water and phenol is decreased because the salt is preferentially soluble in water; this rule is sometime called Timmermans rule [77] (see [89–91] for theoretical modeling). At a fixed temperature the addition of salt lowers the solubility of phenol in the aqueous phase, from 9% without salt to about 5-6% in the presence of molar concentrations of salt (see for instance table 2 in [1]).

4.1.2 Water-phenol nucleic acid mixtures

How can we understand the interaction between phenol and nucleic acids in our system? Clearly, the presence of salt plays a key role, and the polyelectrolyte nature of the nucleic acids must be taken into account [92,93]. Also, we must distinguish between ssDNA and dsDNA. It is well known that phenol interacts better with ssDNA or single-stranded polynucleotides than with dsDNA: Leng *et al.* [18] studied the interaction between phenol and nucleic acids by means of thermal stability, optical activity, viscosity and NMR measurements. They demonstrated that phenol interacts with denatured DNA, poly(A) and poly(U), but poorly or not at all with poly(C) and native DNA. The binding of phenol to single-stranded nucleic acids is therefore also sequence dependent (we will not discuss this aspect in this work). The preferential binding of phenol to denatured DNA rather than to native DNA can also be inferred from studies of the DNA helix-coil transition in the presence of phenol: phenol lowers the melting temperature of dsDNA [10,11,18,94,95]. Another argument is provided by our results: the dsDNA, once formed at the water-phenol interface is expelled in the aqueous phase. This shows that in contrast with the irreversibly adsorbed ssDNA, dsDNA does not interact efficiently with phenol. We will focus our discussion on the interaction of phenol with ssDNA. The behavior of nucleic acids in the presence of mixed solvents is often described using continuous approaches [96,97]. We will examine the outcomes of continuous and discrete approaches for the understanding of phenol-ssDNA interactions, with or without salts. This will show the limitations of continuous approaches. We first briefly recall the polyelectrolyte properties of nucleic acids in aqueous solutions.

In neutral aqueous solutions each phosphate group of the backbone chain of dsDNA and ssDNA is dissociated and carries a negative charge. Nucleic acids are strongly negatively charged polyelectrolytes (see [92,93] for reviews). In the absence of salt, the long-range electrostatic repulsion among the charged phosphate groups tends to destabilize the helical structure of the dilute ds-DNA solutions [92] and to extend ssDNA. In the presence of moderate concentrations of added monovalent cations (typically between 10 mM to 1 M), the range of the electrostatic interaction is screened, and the tertiary structure of dsDNA or ssDNA is altered. Double-stranded DNA has a local standard helical B structure (we neglect here sequence specific effects) and adopts a random or swollen coil conformation at large scale. Single-stranded DNA is much more flexible than dsDNA [98] and can have different types of local structure (helical or disordered). It can fold upon itself in a salt-dependent manner, which results in intrastrand imperfect base pairing [99–101].

4.1.3 Single-stranded DNA-phenol interactions: continuous and discrete approaches

The helical structure of ssDNA is the result of a balance between a destabilizing long-range electrostatic repulsion and stabilizing short-range stacking attractions. This qualitative description of the ssDNA structure suggests that the configuration and the properties of the ssDNA are mainly influenced by electrostatic and polarization forces. Two approaches can be chosen to describe these effects.

a) Continuous approach

– *Without salt*

In this approach the milieu surrounding ssDNA is consider to be homogeneous and continuous. The strength of electrostatic and polarizing forces depends strongly on the ability of the solvent to be polarized. This solvent property is expressed through the dielectric constant of the medium [102]. Water has a high dielectric constant ($\varepsilon_{\text{water}} = 80$) *i.e.* in an external electric field water molecules are easily oriented in the direction of the field. In the close neighborhood of ssDNA the strength of the electric field is important and therefore there exists a shell of oriented water molecules around the DNA molecule [103–105]. The hydration shell will interact with the ssDNAs bases through hydrogen bonding and polarization interactions. Therefore, the strength of stacking between bases should be affected by the quality of solvent-ssDNA interactions [99,106]. Phenol has a dielectric constant much lower than water ($\varepsilon_{\text{phenol}} = 10$ at 60 °C [107]) and is partially miscible in water (9% in volume, at room temperature in the absence of salt). The effective dielectric constant of a phenol saturated water phase in the absence of salt can be estimated using the Clausius-Mossotti equation (also known in optics as the Lorentz-Lorenz equation [102]), and the values given above for $\varepsilon_{\text{water}}$ and $\varepsilon_{\text{phenol}}$. This yields an $\varepsilon_{\text{solution}} = 76.8$ (without salt). Thus, the addition of phenol to the solution decreases the effective dielectric

constant of the aqueous phase. According to Mel'nikov *et al.* this should lead to a weak compaction of the chain [97].

– With added salt

The addition of salt into the solution decreases the amount of dissolved phenol in aqueous phase. At high salt concentrations (in particular at 0.85 M NaCl), we estimate that the percentage of phenol in the aqueous phase has dropped to 5%. This corresponds to an $\varepsilon_{\text{solution}}$ of about 77, close to the value of pure water. The increase of the dielectric permittivity induces a decrease of the local concentration of counterions surrounding ssDNA [93] and increases the Debye screening length. The addition of salt also decreases the range of electrostatic interactions. Under these circumstances, the destabilizing electrostatic repulsion should become less important than the stacking energy between bases that confers to ssDNA its local structure and its stability. Therefore one expects a folding of the ssDNA induced by the stacking the bases, which could involve imperfect intramolecular base pairing as is observed in pure water [99,101]. To sum up, the continuous approach predicts a simple folding of the ssDNA molecule in the presence of phenol and salt, which would enhance intramolecular interactions (imperfect base pairing).

b) Discrete approach

A discrete approach also takes into account forces at the molecular level (short-range effects). We first briefly recall the role of short-range interactions in the structure and stability of nucleic acids.

– Short-range interactions

We will distinguish two types of short-range interactions: stacking and hydrogen bonding. DNAs bases are planar aromatic molecules and can form hydrogen bonds. Bases can interact together by their mutual polarization through a Π-Π interaction. This interaction is called Π-stacking. The competition between the short-range attractive stacking interaction between two adjacent bases and the long-range repulsive electrostatic interaction among the charged phosphate groups of the backbone confers a helical structure to ssDNA and dsDNA. Watson-Crick hydrogen bonding between complementary bases (adenine with thymine and guanine with cytosine) further stabilizes the double-helical structure of dsDNA. The origin of these two short-range interactions (stacking and hydrogen bonding) lies in the capacity of the DNA bases to be polarized. The ability of DNA bases to create hydrogen bonds and the hydrophilic character of the anionic phosphate oxygen imply that water is an integral part of nucleic acid structure [104]. The polymorphism of DNA (ssDNA or dsDNA) is intimately linked to the activity of water [108].

– Without salt

The above description treats the solvent as a continuous medium and does not take into account explicitly the interactions between the water, phenol and the polyelectrolyte. To describe the interaction of ssDNA with phenol molecule it is necessary to take into account its molecular nature. Water is a structured liquid [109]. In the absence of phenol, in the close vicinity of ssDNA, the water molecule network follows the geometry of the polyelectrolyte [110, 111]. The ability of phenol to form hydrogen bonds and its aromatic character allow this molecule to interact with water and to disturb locally the hydrogen network formed among water molecules. The interaction between water and phenol molecules can involve the hydrogen bonding observed in phenol hydrate crystals [83]. In the presence of phenol, the water molecules in the vicinity of ssDNA must now both follow the geometry of ssDNA and interact with phenol molecules. This implies that phenol is in close vicinity of ssDNA. Therefore, it is strongly favorable for phenol molecules to interact with ssDNA, either through a stacking interaction or hydrogen bonding. Phenol indeed increases the solubility of bases [13,14]: this shows the existence of a favorable interaction between phenol and the bases. On the other hand, dioxane and pyridine, two aromatic compounds with low dielectric constants have been shown to decrease the solubility of pyrophosphate [10]. This should also be the case for phenol: it should decrease the solubility of the phosphate backbone. As a result, the interaction of phenol with ssDNA is going to be a subtle balance of factors that either increase the solubility of the bases or decrease the solubility of the phosphate backbone.

The phenol molecule is repelled by the charged oxygen of the phosphate groups but can form a hydrogen bond with the oxygen linked to the phosphorus atom through a double bond. In the absence of salt, the stacking interaction between the bases in ssDNA is destabilized. This favors an intercalation of phenol between two adjacent bases. This could induce a change in the direction and the orientation of the bases with respect to the helical axis. In summary, in the absence of salt, phenol could form a complex with ssDNA involving a stacking interaction, occurring through an intercalation mechanism [112].

– With added salt

The addition of monovalent counterions into the solution changes dramatically this picture. The concentration of dissolved phenol in the aqueous phase decreases as the concentration of added salt increases. Single-stranded DNA is a highly charged polyelectrolyte and the addition of cations into the solution screens the negative charge of the phosphate groups and induces the folding of ssDNA as discussed above. At low salt concentration (below the Manning's threshold [93]), the counterions are trapped along the phosphate backbone of the ssDNA. For ssDNA in the absence of phenol, Manning's threshold (or local counterion concentration near the ssDNA) is equal to 0.21 M [93] (a similar value can be obtained by solving the Poisson-Boltzmann equation). Above Manning's threshold, electrostatic effects become less important. Both the repulsion between the charged phosphate backbone and the phenol molecule and the repulsion between two adjacent phosphates are decreased. Phenol molecules can more
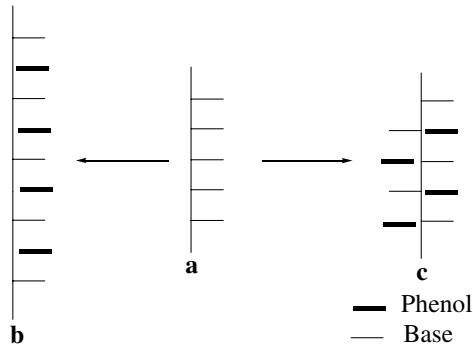
Fig. 11. Schematic drawing of the possible structures of ss-DNA in the presence of phenol molecules. a) ssDNA in the absence of phenol molecules. Bases are stacked together and the distance between two adjacent bases is 3.4 Å. b) A hypothetic intercalated structure of ssDNA in the presence of phenol molecules (distance between two adjacent bases is 7 Å). c) A hypothetic stacked structure, without intercalation, of ssDNA in the presence of phenol molecules.

easily surround the ssDNA chain. The stacking energy between bases is on the order of a few $k_{\mathrm{B}}T$ (Boltzmann's constant k_{B} times the temperature T). In the absence of an electrostatic repulsion, bases can rotate freely around the phosphate backbone and can be stabilized by the phenol molecules present in the vicinity of the ssDNA chain. At this stage, we can only speculate on the conformation of this folded ssDNA: the helical structure of the DNA could be changed either by changing the direction of the helical turn or by having the phosphate backbone at the center with the bases completely exposed to the solvent and stacked with phenol molecules. In support of a stacking interaction, we can mention the results of Leng *et al.* [18]. The authors have shown using proton magnetic resonance that phenol stacks with adenine bases of poly(A) and uracil bases of poly(U). Their experimental system and ours differ (they use a deuterated solution containing 0.11 M phenol and 0.25 sodium cacodylate), but their observation strongly favors a stacking mechanism in our system too. The presence or absence of an intercalating process cannot be inferred from their results. Another argument in favor of a stacking interaction between phenol and ssDNA comes from an analysis of the results obtained with the 13 other organic solvents (discussed below).

Figure 11 summarizes the two structures that we have discussed for a phenol-ssDNA complex: without salt or at low salt, the interaction would require an intercalation process, while at high salt (roughly above 0.2 M, see below), we expect stacking without intercalation. The latter case may be viewed as a phenol-assisted base flipping. These two ssDNA-phenol complexes correspond to different distances between two adjacent bases. The intercalated complex leads to a distance of about 7 Å, while in the second structure this distance could be still that found in B DNA. The existence of such complexes will have to be tested by spectroscopic or microscopic techniques. Remarkably, phenol has been shown to lower the viscosity of poly(A) in the presence of 1 M NaCl [18]: this observation

is not in favor of a simple intercalation mechanism, which should lead to an increase of the viscosity.

The further increase in salt concentration (from 0.3 to 1 M) has two effects: 1) ssDNA folding, 2) expulsion of phenol from the aqueous phase. Both phenol and bases can interact with Na$^+$ through cation-π interactions [19]. Phenol complexed through stacking to the bases becomes expelled from this phase, and this contributes to the transfer of the ssDNA from aqueous phase to the interfacial region between phenol and water.

4.1.4 Conformation of the ssDNA in the water-phenol mixture

a) Conformation in the aqueous phase: an interpretation of the three-dimensional diffusion coefficient of ssDNA

Both fluorobenzene and phenol start to adsorb ssDNA at 0.3 M. This rules out a role for hydrogen bonding and suggests a simple electrostatic mechanism. According to this mechanism, the 0.3 M concentration corresponds to the local counterion concentration C_{loc} near the ssDNA. Using Manning's equation [92,93], we calculate the distance d between two adjacent bases:

$$d = \sqrt{\left[24.3\left(\frac{4\pi k_{\mathrm{B}}T}{q^2 C_{\mathrm{loc}}}\varepsilon_{\mathrm{solution}}\right)\right]}, \qquad (14)$$

where q is the protonic charge. This yields $d = 3.5$ Å, close to the value found in B DNA. This is inconsistent with an intercalation mechanism (a distance of 7 Å would correspond to a concentration $C_{\mathrm{loc}} = 0.08$ M). This simple computation also supports a mechanism involving stacking without intercalation. Let us now try to understand the value of the diffusion coefficient in terms of a conformation of the ssDNA. We use a simple model where the ssDNA is approximated to a sphere of radius R_{G}, the radius of gyration, (to be more exact we should use the hydrodynamic radius of the ssDNA which is proportional to the radius of gyration;. however in a first approximation we consider both radii equal). Using the Stokes-Einstein relation, the diffusion coefficient is equal to

$$D = \frac{k_{\mathrm{B}}T}{6\pi\eta R_{\mathrm{G}}}, \qquad (15)$$

where η is the viscosity of the solvent. We consider that in the experimental condition the viscosity of the aqueous phase is the viscosity of water ($\eta = 0.98 \times 10^{-3}\,\mathrm{kg}\cdot\mathrm{m}^{-1}\cdot\mathrm{s}^{-1}$). From this equation we obtain a radius of gyration of 93 Å. This value can be related to the chain conformation using a simple scaling relation, valid for a flexible chain [113]:

$$R_{\mathrm{G}} \approx \mathrm{d}N^{\nu}, \qquad (16)$$

where d is the distance between two adjacent bases, N the number of monomers (118) and ν is the Flory exponent ($1/3 \leqslant \nu \leqslant 1$) that defines the conformation of the

chain. Combining equations (15) and (16), we derive a Flory's exponent $\nu \sim 0.68$. This value suggests that in the experimental conditions, the ssDNA chain has a swollen conformation. Our result is obviously crude and should only be viewed as indicative of the state of the chain.

b) Conformation of ssDNA chains at the water-phenol interface

What is the conformation of ssDNA chains adsorbed at the water-phenol interface? Answering this question is important for understanding the mechanism of the interfacial renaturation. The conformation of an adsorbed polymer is expected to depend on several factors: the surface chain concentration, the strength of the momomer surface attraction and the reversibility of the adsorption process [114]. When a polymeric chain is adsorbed on a surface, it can retain its three-dimensional conformation if it becomes irreversibly stuck on the surface. On the other hand, if it is able to rearrange freely on this surface, it can also spread and become a two-dimensional polymer, if the attractive energy is high enough. These two extreme possibilities have been described for dsDNA spread on electron micrograph grids [115]. Here, the chains are adsorbed at a liquid-liquid interface, on which they are able to diffuse, and the adsorption is irreversible, indicating a strong adsorption. These facts suggest that the adsorbed ssDNA chains are flattened and can be considered as two-dimensional polymers. One can envision the chains with their bases immersed in the phenolic phase, while the phosphate backbone and the sugars remain in the aqueous phase. There exist several possible simple conformations for the adsorbed ssDNA chain: globular (swelling exponent $\nu = 1/2$), swollen coil ($\nu = 3/4$), or extended rod ($\nu = 1$). An adsorbed chain can be viewed as a disk of radius R_1 and occupies a surface $\pi(R_1)^2$. From this surface one can define an overlap concentration C^* corresponding to the close packing of such disks. In the experiment where we renature DNA without shaking, renaturation becomes slower than adsorption when there remains about 0.47 ng of adsorbed 118− (corresponding to a release of about 20% of the adsorbed material; see Fig. 8b). Now the onset of the decrease of the rate of renaturation should occur for a surface concentration close to the overlap concentration C^*. We can therefore use this experiment to guess the conformation of the adsorbed chain. For a globular conformation, ($R_1 = 0.5 \times 3.5 \times (118)^{1/2} = 19$ Å), we obtain $C^* = 580$ ng/cm^2, corresponding to an amount of chains of 58 ng on the interface. Assuming as swollen coil conformation ($R_1 = 0.5 \times 3.5 \times (118)^{3/4} = 62.6$ Å), we obtain $C^* = 50$ ng/cm^2, corresponding to an amount of chains of 5 ng. Finally, for an extended rod ($R_1 = 206$ Å), we obtain $C^* = 5$ ng/cm^2, corresponding to an amount of chains of 0.5 ng on the interface, very close to the value of 0.47 ng mentioned above. This simple reasoning suggests that the chains have an extended, rodlike structure at the interface. It is worth noting that a similar conclusion would still hold if we assume an intercalating mechanism (leading to a monomer size of 7 rather than 3.5 Å). Indeed,

with an intercalated chain having a swelling exponent ν ($R_1 = 0.5 \times 7 \times (118)^{\nu}$ Å), the close packing of 0.47 ng of ssDNA is obtained with $\nu \approx 0.85$, implying an extended structure.

4.1.5 Comparison of phenol with other simple organic compounds: roles of hydropohobicity and aromaticity

In addition to phenol, we have tested 13 organic solvents for their capacity of adsorbing ssDNA at the water-organic solvent interface at room temperature in the presence of NaCl. We will now compare our results with those reported in the literature, and discuss them in terms of hydrophobic and aromatic interactions. The interaction of simple organic compounds with DNA has been described by several authors [10,12,17]. These authors have concluded that simple organic compounds interact with ssDNA mainly through a hydrophobic interaction, but the situation is actually more delicate.

According to Kauzmann [9], a hydrophobic interaction has a small and positive enthalpy variation and a large and postive entropy variation. In contrast, a stacking interaction between two planar aromatic compounds is not as a role entropically driven. Base stacking, for instance, is associated with a negative enthalpy and a negative entropy variation [15,116]. In other words, in water, it is more favorable for monomeric bases to form a stacked self-associated structure rather than to be excluded from water [13]. This suggests that the description of ssDNA-organic compounds using a simple hydrophobic interaction must be carefully examined.

Levine, Gordon and Jencks [10] studied 54 organic compounds for their capacity to lower the melting temperature of dsDNA (destabilization of dsDNA in the presence of 0.04 M salt followed at 75 °C). They came to the conclusion that the decrease of the melting temperature of dsDNA by these compounds is due to their preferential binding to ssDNA. The 6 most efficient compounds in their test were phenol, p-methoxyphenol, benzyl alcohol, aniline (four organic solvents) plus pyridine and purine. These six compounds are polar, planar, aromatic molecules. Levine, Gordon and Jencks concluded that the most efficient interaction with single-stranded nucleic acids is a hydrophobic interaction. They did not rule out a special mechanism for the action of aromatic compounds in their assay, but considered that this mechanism would be a minor contribution to an overall hydrophobic effect. In a similar study Ts'o and coworkers [11] examined 16 organic compounds for their capacity to lower the melting temperature of dsDNA or poly(A) and obtained similar results: their most efficient compounds were polar, planar, aromatic molecules such as purine, purine derivatives or phenol. Helmer, Kiehs and Hansch [12] analyzed the data of Levine *et al.* [10] by looking for correlations between octanol-water partition coefficients P of the compounds and their capacity to lower the melting temperature of dsDNA. They found that for the 12 alcohols and phenols as well as for the 5 amides used by Levine *et al.* there exist a good linear relationship between $\log(C)$ (where C

is the molar concentration of the compound required to obtain 50% denaturation of dsDNA at $73\,°C$ in the work of Levine *et al.*) and $\log(P)$. From these results they too concluded that these compounds act through hydrophobic interactions in the sense of Kauzmann.

The most efficient organic solvents in our adsorption assay are also all planar, aromatic, compounds. The three most efficient compounds are phenol, guaiacol (o-methoxyphenol) and fluorobenzene. Strikingly, phenol is the most efficient compound in these two very different assays. This underlines the efficiency of phenol as a ssDNA ligand. The most efficient compounds in the two assays are all planar, aromatic, polar molecules. The aromaticity of these compounds is therefore essential for an optimal interaction with single-stranded nucleic acids. Whether the interaction of ssDNA with these aromatic compounds is a typical (entropically driven) hydrophobic interaction will require further studies.

Aromaticity is of course not the only requirement. The presence of a hydroxyl group on the aromatic ring is also required, as witnessed by 1) the better efficiency of phenol over fluorobenzene at high salt concentrations and 2) the presence of two substituted phenols (o- and p-methoxyphenol) in the best performing compounds of the two assays. We conclude from these studies that the most efficient ssDNA binding compounds are planar, aromatic molecules and that phenol is the most efficient binding compound in these very different assays.

4.1.6 Renaturation at the water-phenol interface

We now discuss the mechanism of DNA renaturation at the water phenol interface.

Topological issues in the interfacial renaturation

The adsorption at the water/phenol interface is expected to lead to a reduction of dimensionality from 3 to 2 for the ssDNA chain: this is the flattening discussed above. In that case, the topological constraints imposed by the reduced dimension of the interface could prohibit the formation of a complete helical structure of the dsDNA at the interfacial region. According to this hypothesis, when two complementary ssDNA encounter at the water-phenol interface, only a short (less than a full turn of the helix) double-stranded DNA segment is formed and at once transferred to the aqueous phase; the further growth of the double helix occurs at the same time as a transfer of the remaining ssDNA segments (Fig. 12). The growth of the double helix in the aqueous phase is coupled with a two-dimensional translation and a rotation of the ssDNA segments. The adsorption of the extremities of ssDNA at the interface can prevent the topological entanglement of the two complementary chains during the annealing process. This could explain the efficiency of PERT in the renaturation of long DNA chains (even tens of kilobase long [1,3]). On the other hand, we note that even if the interface can accommodate a completely helical double stranded DNA,
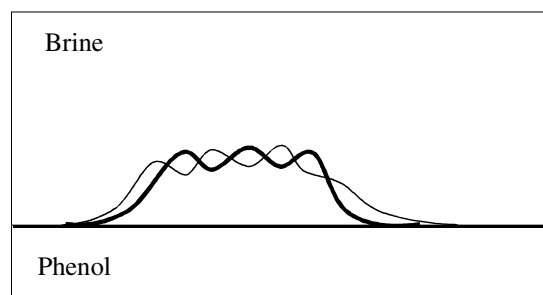

Fig. 12. A hypothetic transient structure formed during the interfacial renaturation. As two portions of two complementary ssDNAs encounter each other a double helix is formed. The double-helical portion (assumed here to have started inside the ssDNAS rather than at one extremity) is progressively expelled from the water-phenol interface to the aqueous phase. The single-stranded portions still remain adsorbed at the interface.

dsDNA is not expected to remain at this interface, since it partitions entirely in the aqueous phase in our system: the adsorption of dsDNA is not expected to be long lived.

The interfacial mechanism of PERT

As we have seen in the introduction, the basic mechanism of PERT, in particular the location of the nucleic acids in the two-phase system has remained poorly understood. According to Kohne *et al.* [1], "*The single-stranded DNA may be concentrated at the phenol:aqueous interface or by forming aggregates or semiprecipitates elsewhere in the two-phase system*". Other authors have favored the idea that the reassociation of nucleic acids takes place at the water-phenol interface, but were not able to exclude an aggregation/condensation mechanism [2,3,117]. Our results obtained for extremely dilute ssDNA solutions establishes that PERT is an interfacial reaction. The complementary ssDNA are associated with phenol droplets when they renature. They are stably adsorbed at the surface of such droplets until recombination occur. We have shown that the interfacial adsorption is a monomolecular event in the absence of shaking. This result does not exclude the existence of aggregates in the aqueous phase either in the presence of shaking or at higher DNA concentrations.

The role of shaking

We have confirmed that shaking is necessary to obtain high reaction rates. The role of shaking is twofold. 1) It reduces the time required for the chains to reach the interface. 2) It greatly expands the interfacial area. We can give a rough estimate of this expanded interfacial area. We notice that the emulsion is turbid. This scattering of visible light implies that the size of the scattering centers is in the micrometer range. A volume of 40 μl of phenol corresponds to about 10^{10} droplets with a radius in the micrometer range. This number is to be compared to the

number of ssDNA chains (1.6 pM in 100 μl, about 10^8 chains). The emerging picture is that there is a small portion of phenol droplets (about 1%) that carries a ssDNA chain. The annealing of complementary chains can only occur during the coalescence of two droplets.

As mentioned in the introduction, the rate of renaturation is independent of the length of the complementary strands at very low DNA concentrations (where the highest renaturation rates are obtained) [1,2]. The picture provided above for the mechanism of PERT in this case (where each chain is carried by an individual phenol droplet) suggests a simple explanation for this observation. The rate would be determined by the dynamic properties of these droplets and by their coalescence rather than by the chains themselves.

Hydrodynamics of PERT

The PERT reaction involves the "vigorous shaking" of the water/phenol biphasic solution. The paragraph above implies that PERT depends in a crucial manner on the hydrodynamic field. The stability of the obtained microemulsion depends strongly on several parameters. The shape and the size of phenol droplets are defined by the combined action of the salt concentration and the rate of coalescence between phenol droplets. By considering the Laplace-Young theory of capillarity, the shape and the size of the phenol droplets can be linked to the interfacial tension between water and phenol and to the difference between the densities of the two bulk phases. The salt concentration influences not only the interfacial tension between water and phenol, but also the difference between their bulk densities. The diffuse ion layer (or Stern layer) that surrounds the phenol droplet depends on the salt concentration and could be one of the phenol microemulsion stabilizing factors. The coarsening rate of the mist of phenol droplets could be driven solely by salt concentration, if the mechanism of encounter between droplets were diffusion-controlled [118]. However, because of the shaking, the flow is turbulent. The frequency of contacts between particles in such a flow increases substantially in comparison with the number of encounters in a motionless fluid. In addition, the frequency of encounters between droplets is not solely a function of the strength of shaking. For small enough particles (size of the particle smaller than the extent of the turbulent flow) there always exists a region where the Brownian diffusion predominates over the turbulent diffusion [76]. Therefore, the frequency of encounters between phenol droplets will depend ultimately on both the strength and the frequency of the shaking, and also on the salt concentration, which determines the average size and shape of the droplets.

4.2 Comparison with other renaturating approaches

We will now compare the mechanism of this interfacial renaturation (with or without shaking) with other renaturation reactions. We distinguish three lines of investigation, which we describe now in detail.

4.2.1 Thermal renaturation

The physical chemistry of nucleic acid annealing has been first studied *in vitro* in well-defined conditions using either synthetic polynucleotides [21,22] or DNA [20,23,24]. In all these works the reactions were investigated using dilute nucleic acid aqueous solutions in the presence of monovalent cations. This approach is called thermal renaturation. The rationale behind this choice was to try to avoid nucleic acid aggregation [119]. As a result, thermal renaturation takes place in the bulk of a homogeneous aqueous phase. These classic investigations led to the conclusion that the reactions are thermally activated (hence their name), and proceed through a nucleation and growth mechanism [120]. Monovalent salts have two effects; they increase the melting temperature of DNA (stabilize the dsDNA form) and increase the rate of renaturation (by lowering the electrostatic repulsion between complementary ssDNA). Salt concentration effects can be understood using appropriate laws of mass action [92,93]. These equations predict power law relations between salt concentration and the melting temperature or the renaturation rate, and such relations are observed experimentally [23, 92,93]. At elevated temperature, the rate of renaturation grows as the square root of the length of the complementary strands in the thermal renaturation of DNA [24]. This is another example of a law of mass action behavior, where the square root exponent can be understood as an excluded-volume effect reflecting the statistics of internal contacts in the ssDNA chains [121]. At physiological temperatures (25–37 °C), annealing in the presence of monovalent salt is inefficient for long ssDNA, because of imperfect intramolecular base pairing [23,99]. One way to overcome this difficulty is to add organic solvents such as formamide or dimethyl sulfoxide in the solution [96,117]. In a variant form of thermal renaturation, one of the complementary strands is immobilized on a solid surface [117]. The effect of this immobilization is to reduce the rate of the reaction compared to the bulk situation.

4.2.2 Renaturation in the presence of condensing agents

In a second line of investigation, a link between DNA renaturation and nucleic acid condensation was established [3]. It has been shown that many simple compounds (incompatible polymers, polyamines, multivalent cations, cationic surfactants) that condense (*i.e.* collapse or aggregate) nucleic acids can also greatly accelerate DNA renaturation. As for monovalent salts, the addition of such condensing agents also increases the melting temperature of dsDNA [25,122,123]. In the presence of the condensing agent, DNA renaturation takes place at the same time as the aggregation of the nucleic acids (single-stranded and double-stranded DNA) present in the solution [8]. Renaturation of condensed nucleic acids can be kinetically first order or second order, depending on the nucleic acids concentration. Renaturation of extremely dilute nucleic acids condensed by spermine [8] can occur at rates compatible with a diffusion-controlled bimolecular reaction [118]. The

polyamines lower the electrostatic repulsion between the ssDNAs. It leads to large rate increases (25000 fold) at room temperature for small DNA chains (about 100 base pairs). The efficiency of the reaction decreases sharply for longer chains, because the intramolecular folding of the ss-DNA greatly diminishes their accessibility [3,25]. In contrast with thermal renaturation, salt concentration effects on the rate of the reaction cannot be described using the law of mass action [3,8]. Also in contrast with thermal renaturation, the rate of renaturation has a weak temperature dependence (as expected for a reaction operating close to the diffusion control limit).

4.2.3 Renaturation in the presence of SSBPs

In a third line of investigation, single-stranded nucleic acid binding proteins (SSBP such as the gene 32 protein of bacteriophage T4 [26], RecA protein [27] or the *Escherichia coli* single-stranded binding protein (*Eco* SSB [28]) were purified and shown to be able to accelerate these reactions both under physiological temperatures and for long DNA. Many other single-stranded nucleic acid binding proteins have since shown to possess this activity. These proteins are often involved in genetic recombination [30], but also include various proteins such as the nucleocapsid protein of the human immunodeficiency virus I [32] and the prion protein [34]. Single-stranded nucleic acid binding proteins facilitating nucleic acid annealing are often referred to as nucleic acid chaperones [29]. Nucleic acid chaperones are generally essential to life [33].

The interactions of nucleic acid chaperones with nucleic acids and the mechanisms by which they accelerate their annealing are subtle, and can differ from one protein to another. Nevertheless, two general (non-exclusive) mechanisms have been described, which seem to account for some of the properties of several of these proteins. The first mechanism (A) involves the preferential interaction of the proteins with single-stranded nucleic acids, an interaction that greatly relies on aromatic amino acids; the second mechanism (B) involves the aggregation of single-stranded nucleic acids.

A) Nucleic acid chaperones bind, in general, preferentially to ssDNA rather than to dsDNA. Thus, in contrast with the monovalent salts or the simple condensing agents mentioned above, nucleic acid chaperones usually lower rather than increase the melting temperature of DNA. Furthermore, they stabilize single-stranded nucleic acids in an unfolded conformation. The removal of the imperfect secondary structure is presumably favorable for later annealing. A striking example is provided by the interaction of protein RecA with ssDNA [30,124]. Numerous experimental studies have shown that aromatic amino acids (phenylalanine, tryptophan and tyrosine) play an essential role in the interaction between SSBPs and single-stranded nucleic acids [124–128]. The interactions between these amino acids and the nucleic acids can involve stacking interactions (with or without intercalation, as schematized

in Fig. 11), but also other interactions such as hydrogen bonding or cation-π interactions [19]. The interactions between SSBPs and single-stranded nucleic acids fall in two categories. In the first category, the nucleic acids are immobilized on the protein surface. This can be observed in crystal structures of complexes between single-stranded nucleic acids and SSBPs, for instance for *Eco* SSB [127]. The immobilization involves stacking interactions of aromatic residues on the nucleic acid bases. In the second category, the nucleic acid bound to the SSBP is still mobile. This has been seen for instance in the crystal structure of T4 gp32 complexed with an oligonucleotide (p(dT)6) which shows that the ssDNA is diffusing on the aromatic acid residues of the protein surface [126]. Remarkably, depending on the experimental conditions, *Eco* SSB can form immobile or mobile complexes with ssDNA: mobile complexes have has been observed by NMR experiments [129].

B) Aggregation processes stimulate some of these proteins. It was proposed that the condensation of single-stranded nucleic acids also accounts (at least partially) for the acceleration of base pairing reactions by nucleic acid chaperones [3]. Several nucleic acid chaperones have in fact been shown either to act as condensing agents, such the *Escherichia coli* RecA protein [5, 130], the protein NCP7 of HIV-1 [131,132] or the prion protein [133], or to have an enhanced annealing activity in the presence of condensing agents [5,28]. These studies were usually performed at such DNA concentrations that the aggregation process was fast and the renaturation reaction kinetically first order.

4.2.4 Comparison of PERT with the three lines of investigations: homogeneous and heterogeneous reactions

Table 2 provides the values for the rate of annealing reactions of different nucleic acids in various conditions. The rate constants have been expressed using ssDNA chain molar concentrations [3]. Note that phosphate molar concentrations have usually been employed to express these rates [1,23–26,28,117]. The use of chain concentrations allows a direct comparison of the constants obtained in the different experiments and also a direct comparison with the value expected for a diffusion-controlled process. The bimolecular rate constants span six orders of magnitude. The lowest rate constant, 4×10^4 $M^{-1}s^{-1}$, corresponds to the highest rate that can be obtained at room temperature in a dilute aqueous solution in the presence of monovalent cations for a long DNA molecule (T7 DNA, 40 kb long [23]). In an aqueous solution, this rate can be greatly increased by raising both the temperature and the monovalent salt concentration (leading to a value of 1.2×10^8 $M^{-1}s^{-1}$ at 65 °C, 0.5 M NaCl). This large temperature dependence is the hallmark of thermal renaturation, and contrast with the weak temperature dependence of PERT. At the other extreme, the highest value is obtained using PERT with very dilute DNA solutions (see [1], and this work). The rate constants obtained with PERT in these conditions do not depend on the length of the DNA

Table 2. Bimolecular rate constants of DNA renaturation in various experimental conditions.

Nucleic acid	Reaction medium	Temperature	k_2 $(\mathrm{M^{-1}\,s^{-1}})$	Reference
Intact Phage T7 DNA (39.9 kb)	0.1 mM buffer, pH 8 40 mM NaCl	25 °C	4×10^4	Studier (1969) [23]
Intact Phage T7 DNA (39.9 kb)	0.1 mM buffer, pH 8 60 mM NaCl	35 °C	6×10^5	Studier (1969) [23]
Intact Phage T7 DNA (39.9 kb)	0.1 mM buffer, pH 8 0.5 M NaCl	65 °C	1.2×10^8	Studier (1969) [23]
Phage T4 DNA (168.9 kb) ~ 16 kb long fragments	20 mM buffer, pH 7.6 10 mM KCl 40 mM $MgSO_4$ gp32 (in excess over DNA)	37 °C	1×10^8	Alberts and Frey (1970) [26]
Intact Phage λ DNA (48.5 kb)	10 mM buffer, pH 5.5 10 mM NaCl 10 mM $MgCl_2$ *Eco* SSB (1.2-fold excess over DNA)	37 °C	1.6×10^7	Christiansen and Baldwin (1977) [28]
Intact Phage λ DNA (48.5 kb)	10 mM buffer, pH 5.2 20 mM NaCl *Eco* SSB (10-fold excess over DNA) 2 mM spermine	37 °C	3.4×10^8	Christiansen and Baldwin (1977) [28]
118 bp DNA fragment from Phage ϕX 174	10 mM Tris HCl 1 mM EDTA 0.46 mM spermine	25 °C	1.4×10^9	Chaperon and Sikorav (1998) [8]
124 bp DNA fragment from pSV2gpt	50 mM NaCl 1 mM CTAB	68 °C	6×10^9	Pontius and Berg (1991) [25]
E. coli DNA 0.5 μg/ml	PERT, 2 M LiSCN	22–24 °C	4.2×10^{10}	Kohne *et al.* (1977) [1]
118 bp DNA fragment from Phage ϕX 174	PERT, 0.85 M NaCl	22–24 °C	4.2×10^{10}	This work

chains: we can therefore directly compare these rates with those obtained for T7 DNA at room temperature [23]. We conclude that for long DNA chains, PERT can increase the rate of renaturation by a million-fold at room temperature. This rate acceleration is much larger than estimated earlier by Kohne *et al.* (an acceleration of "*many thousand times*" as mentioned in the introduction; this is because these authors compared the rate obtained with PERT with a rate obtained at an elevated temperature).

The comparison of these different rates in Table 2 requires care. The rate of PERT is measured under strong mixing conditions, whereas in the other experiments the samples are not stirred. For unstirred reactions, the theory of Smoluchowski [118] can be used to estimate the rate constant expected for a diffusion-controlled reaction, about 6×10^9 $\mathrm{M^{-1}\,s^{-1}}$. The rate constants obtained in the presence of various DNA condensing agents (polyethylene glycol [3], spermine [8], cetyltrimethyl ammonium bromide or CTAB [25]) are high enough to be compatible with a diffusion-controlled reaction in a dilute DNA solution. A diffusion-controlled base-pairing reaction with modified bases in chloroform has been reported by Hammes and Park [134]. Similar rates were obtained in the case of this simpler reaction.

The absolute value obtained for the rate constant using PERT is quite striking. Not only does PERT outperform the catalytic capacities of the single-stranded nucleic acid binding proteins gp32 and *Eco* SSB; the rate constant for PERT is also almost ten times faster than the Smoluchowski value predicted for a diffusion-controlled reaction. It is close to the value reported for the fastest (and much simpler) known bimolecular

reaction, namely the recombination of H$^+$ with OH$^-$ (1.3×10^{11} M^{-1}s^{-1}; [135]). This also shows that one can obtain rates that exceed a diffusion-controlled limit under appropriate mixing conditions. While such a conclusion is common knowledge in chemical engineering [136], we feel that it is not the case in molecular biology, where one often gets the impression that no process can be faster than a diffusion-controlled one. It is not generally appreciated, for example, that molecular motors can increase chemical rates beyond the diffusion-controlled limit (we plan to discuss this issue elsewhere). In PERT, the very fast rates require vigorous shaking. This shaking may be seen as a rudimentary version of the present-day more sophisticated molecular motors.

The presence of DNA condensing agents leads to a more complex situation. As a rule, dsDNA condensing agents lead ultimately to an aggregation of dsDNA [137]. This means that the field of dsDNA condensation at large belongs to heterogeneous chemistry. Furthermore, dsDNA condensing agents can also act as ssDNA condensing agents. In the presence of spermine, for instance, DNA renaturation takes place at the same time as the aggregation of both ssDNA and dsDNA chains present in the solution [8]. We are not dealing with a simple reaction occurring in the bulk of a homogeneous aqueous solution, but rather with a reaction taking place at the same time as a phase separation. This remark points to a common feature between PERT and the reactions taking place in the presence of condensing agents. In both cases, the reactions do not occur in the bulk of a homogeneous phase, in contrast with the standard (thermal) renaturation. In both cases also (adsorption using PERT or aggregation with condensing agents), the volume available to the ssDNA chains is decreased and their effective concentration is increased, contributing to raise the rate of the reaction.

We, therefore, see that in Table 2 the concepts of homogenous chemistry can be used to account for the lowest rates (thermal DNA renaturation data of Studier [23]), whereas the highest rates come within the province of heterogeneous chemistry. The catalysis of renaturation by SSBPs corresponds to an intermediate situation in two aspects. 1) Homogeneous *versus* heterogeneous chemistry. Renaturation in the presence of condensing agents or the water-phenol two-phase system involves several macroscopic phases (DNA rich phases, phenol rich phase, phenol droplets of micron sizes). Renaturation in the presence of SSBPs involves the interaction of DNA with proteins of colloidal size. 2) Renaturation rates. The catalysis by SSBPs leads to rate constants that are faster than those obtained in the presence of monovalent cations at "physiological" temperatures (25–35 °C), but smaller than those obtained with DNA condensing agents or with PERT. Note that the addition of the condensing agent spermine increases the efficiency of *Eco* SSB (increasing the rate constant by a factor 20 [28]). This is likely to decrease the electrostatic repulsion between the ssDNA; whether this involves the condensation of the ssDNA chains is not known.

4.2.5 Similarities between renaturation at the water phenol-interface and the renaturation in the presence of nucleic acid chaperones

The mechanism of renaturation at the water-phenol interface (with or without shaking) contrasts with the standard thermal renaturation of nucleic acids in several respects such as temperature, chain length and salt concentration dependence. On the other hand, there exist striking similarities between this interfacial reaction and the mode of action of SSBPs:

1) Adsorption

   Both in this interfacial reaction and in the catalysis by SSBPs, the ssDNA chains must be adsorbed to a surface of the SSBP to react (the surface of the protein or the water-phenol interface).

2) Preferential binding to ssDNA and stabilization of ssDNA

   Phenol and SSBPs both bind preferentially to ssDNA. As a consequence, both phenol and (most) SSBPs lower the melting temperature of dsDNA. Aromatic residues of SSBPs play a key role in this preferential binding, as explained above. Remarkably, phenol stabilizes ssDNA at the water-phenol interface in an extended conformation, close to rodlike. This is reminiscent of the stiffening of ssDNA in the presence of RecA [138]. A stabilization in an extended form (which in the case of RecA also leads to a stretching of the ssDNA) is likely to contribute to the efficiency of the annealing reaction in the two systems.

3) Renaturation of long DNA chains

   In contrast with simple condensing agents [3,25], both PERT [1,3] and SSBPs (see Tab. 2) can fully renature very long DNA chains (tens of kilobase long).

4) Turnover

   Both in the interfacial renaturation and in the renaturation in the presence of an SSBP, the formation of the double-stranded product of the reaction leads to a dissociation event: in the first case, the dsDNA is desorbed from the water-phenol interface; in the latter, the SSBP dissociates from the dsDNA. This allows the reactions to turnover.

5) Surface diffusion of ssDNA

   The ssDNA chains can diffuse on the water-phenol interface. Single-stranded DNA oligonucleotides can also diffuse on the surface of different SSBPs [126, 129], Furthermore, in the case of gp32, this diffusion largely relies on tyrosine residues [126]: thus both PERT and this protein make use of phenolic groups to provide the diffusive motion. In the case of *Eco* SSB, the interaction is more complex, involving other aromatic residues. In addition, this protein can have various modes of binding, some of which lead to immobile ssDNA-protein complexes [31]. We note that the surface diffusion of acetylcholine on the surface of acetylcholinesterase has been proposed to contribute to the high catalytic rates of this enzyme,

and that this diffusion would also take place on a layer of aromatic residues [139]. It has been proposed in this case that the aromatic side chains shield the direct electrostatic interactions between the substrate and the enzyme.

6) Dehydration of ssDNA

Both in the water-phenol two-phase system and in catalysis by SSBPs, the ssDNA chains are dehydrated. Phenol stacking causes dehydration in the bulk of the aqueous phase, and the interfacial location further contributes to dehydrate the ssDNA. Extensive dehydration is also observed in complexes between double- or single-stranded nucleic acids and proteins [140].

7) Salt concentration effects

Both in PERT and in catalysis by SSBPs, increasing salt concentration does not lead to a simple law of mass action behavior, but to a more complex, cooperative effect. The existence of a coupling between adsorption and renaturation in PERT provides a plausible explanation for the observed critical dependence of the renaturation rate on the salt concentration [3]. Indeed, the coil-helix transition should be roughened by a coupling with an adsorption process [35,36,141]. This offers a plausible explanation for the observed breakdown of the law of mass action behavior. A similar reasoning [142] can be used to explain the salt effects in the case of a coupling between renaturation and a coil-globule transition in the presence of condensing agents [3]. In both cases, the breakdown of the law of mass action is an indication of the heterogeneity of the system. For SSBPs, the situation is clearly much more complex [31]. The results obtained with PERT suggest however that part of the cooperative effects seen with salts in the interactions between ssDNA and SSBP has its origin in the adsorption of the nucleic acids by these proteins.

4.2.6 Comparison with other systems involving surface diffusion processes

In this work, we have studied a surface reaction involving extremely dilute DNA solutions. We have modeled this problem as a problem of gaseous adsorption (neglecting interactions between similar DNA chains), in the spirit of early studies on the adsorption and diffusion of gases on solid surfaces. The concepts we have used (Eley-Rideal *versus* Langmuir-Hinshelwood mechanisms) are standard concepts of surface chemistry, applied here to the case of polymeric chains. The issue of diffusion on surfaces (mostly on solid surfaces) and its role in chemical processes was already considered in detail by several authors before World War Two [70,143,144]. In 1968, Adam and Delbrück (apparently unaware of these earlier works) published an influential theoretical article on the role of reduction of dimensionality in biological processes [145]. They showed that diffusion-controlled reaction rates between two reactants could be enhanced through a reduction of dimensionality of the reaction space (and in addition in-

vestigated the role of convection in such processes). It has been suggested that the work of Adam and Delbrück could help to understand the mechanism of PERT [3]. Other authors have also used the work of Adam and Delbrück for describing different biological and technological systems [75,146]. Chan, Graves and McKenzie in particular have suggested in a theoretical work that the rate of DNA hybridization on a solid surface could be increased by surface diffusion [147].

A typical scheme that Adam and Delbrück considered involves: *"Stage I, free diffusion* (of the probe molecule) *in three dimensions to a specially designed surface (interface) in which the target is embedded. Stage II, diffusion on this surface. We imagine the molecule to be held on this surface by forces sufficiently strong to guarantee adsorption but also sufficiently weak to permit diffusion along the surface."* Note that the scheme Adam and Delbrück consider implies an irreversible adsorption of the probe molecule (although Adam and Delbrück do not state this point explicitly). Adam and Delbrück compare two hypothetical diffusion processes towards the target: a direct three-dimensional search, and a surface diffusion process. To do so, they compute the mean time of diffusion $\tau^{(i)}$ to a small target of diameter α within a large diffusion space of dimensionality i and diameter β, and establish the following theorem:

$$\tau^{(i)} = \frac{\beta^2}{D^{(i)}} f^{(i)} \left(\frac{\beta}{\alpha} \right) , \qquad (17)$$

where $D^{(i)}$ is the diffusion coefficient of the molecule in the space of dimensionality i, and $f^{(i)}(\alpha/\beta)$ (called the tracking factor) is shown to depend strongly on the dimensionality:

$$\tau^{(3)} \approx \frac{\beta^2}{D^{(3)}} \frac{\beta}{3\alpha}$$

and

$$\tau^{(2)} \approx \frac{\beta^2}{D^{(2)}} 1.15 \, \log \frac{\beta}{\alpha} \qquad \text{for} \quad \alpha/\beta \ll 1 . \qquad (18)$$

These equations show that a probe can theoretically greatly speed up the overall process of diffusion toward its target by performing part of the diffusion on the surface, instead of reaching the target directly by diffusion through the three-dimensional space, provided that the ratio $D^{(2)}/D^{(3)}$ is not too small. If the probe then reacts with its target, it can be seen that the combined three and two-dimensional search described by Adam and Delbrück corresponds to a Langmuir-Hinshelwood mechanism (and the direct three-dimensional search to an Eley-Rideal mechanism). Adam and Delbrück discussed the biological implications of their theorem (assuming ratios $D^{(2)}/D^{(3)} > 10^{-2}$), and suggested that surface diffusion processes have contributed to the evolutionary advantages of biological (internal) membranes.

The experimental realization of Adam and Delbrück's scheme is not obvious: how can one obtain an efficient surface diffusion, without dissociation, in particular when

the adsorbed molecule is a polymer? The following analysis suggests that a key criterion is the fluidity of the interface. The adsorption of a polymer on a surface can be described by a model assuming the trapping of monomers in potential wells. The shape and the depth of these potential wells depend on the surface profile. If the surface is a solid, the motion of the adsorbed polymer requires multiple desorption events (corresponding to the escape from the potential well). This suggests that the polymer mobility will decrease exponentially with its length (solid friction). On the other hand, if the interface is fluid (a liquid-liquid interface as here, or a fluid lipid surface), the mobility of its constituents can assist the transport of the polymer. This crude view suggests that in these circumstances the friction exerted on the chain will increase linearly with the size of the polymer (Rouse friction), in contrast with the exponential increase expected on the solid surface. Note that this is a delicate issue, and that other models can be thought of to describe the surface diffusion of a polymer [148].

There exist plausible illustrations of these two types of mobility in the literature. 1) There are many examples of a greatly reduced mobility for polymeric chains adsorbed on solid surfaces, suggestive of a solid friction. Guthold *et al.* [149], for instance, have studied the diffusion of dsDNA restriction fragments deposited on mica. For a 1 kilobase pair fragment, they measure a diffusion coefficient D_{2d} that is 10^{-6} smaller than D_{3d} (7×10^{-14} cm^2 s^{-1} *versus* 5.4×10^{-8} cm^2 s^{-1}). 2) An illustration of the fast dynamics of polymeric chains at a fluid interface has been reported by Maier and Rädler [150, 151]. These authors have studied the two-dimensional diffusion of dsDNA molecules on glass-supported cationic lipid membranes, and found that it follows Rouse dynamics. For a 1 kilobase pair fragment, they measured a diffusion coefficient D_{2d} of about 4×10^{-10} cm^2 s^{-1} which is much larger than the D_{2d} diffusion coefficient measured by Guthold *et al.* [149] for a DNA of the same size. For an 80 base pair fragment, they measured a diffusion coefficient D_{2d} of about 4×10^{-9} cm^2 s^{-1} close to the value that we obtain for the $118-$ ssDNA chain (3.9×10^{-9} cm^2 s^{-1}). We conclude from these two examples that for polymeric chains, the scheme of Adam and Delbrück is most efficiently realized when the interface has a liquid-like structure. The interface can be a simple liquid-liquid interface, or the surface of a membrane. There is, however, a difference between the two systems: in the adsorption on cationic lipid membranes, the chains are hold by electrostatic forces at low salt concentration, and the adsorption becomes reversible above 70 mM, in contrast with the water-phenol system.

Another related issue is that of the diffusion of proteins of the surface of DNA [152–155]. While this diffusion is commonly described as a one-dimensional process, it appears more realistic to consider it as two-dimensional one (because the DNA double helix has a finite width). It seems likely that the flexibility of both the DNA and the protein will contribute to the efficiency of the diffusion process. One way to test this hypothesis would be for instance to investigate the effect of the surface con-

finement of a DNA chain on the diffusion of the bound protein along it [149]. Another investigation would be to probe the length dependence of DNA mobility on proteic filaments such as RecA filaments [30] to see if they follow a Rouse dynamics.

4.3 Implications for partitioning studies

4.3.1 Implications for the partitioning of nucleic acids in water-phenol systems

The purification of nucleic acids in two-phase systems (water-chloroform, water-phenol or water two-phase systems) is one of the most common techniques of molecular biology [37–45]. Most DNA extraction protocols have been designed for dsDNA (with the notable exception of the work involving ssDNA bacteriophages [41]). The goal of an extraction procedure is to provide intact nucleic acids, free of contaminants such as proteins or lipids. Phenol extraction is generally thought to be more efficient than chloroform extraction [47], probably because proteins partition completely in the phenolic phase [46, 156]. However, phenol alone is often unable to disrupt complexes between nucleic acids and proteins, and added salts are required to obtain this disruption [157]. This observation suggests that phenol is more a solvent than a denaturing agent for some proteins. Phenol alone is for instance often unable to inhibit RNase activity. Therefore, phenol is often used in combination with a potent protein denaturant (guanidinium thiocyanate) to obtain intact RNA [158, 159].

Our results have implications for the use of water-phenol extraction procedures in the isolation of DNA. Earlier studies reported losses of dsDNA (especially A-T rich DNA) due to denaturation and "aggregation" at the water-phenol interface [52–55]. It was also shown that at low pH dsDNA is denatured and that the denatured ssDNA is transferred to the phenolic phase [46, 49]. We have shown that a complete removal of single-stranded DNA material from the aqueous phase can occur because of its adsorption at the water-phenol interface. This adsorption does not require an aggregation process and does not necessitate a massive transfer of the nucleic acids in the phenolic phase, as is observed at lower pH. This suggests that in partitioning studies, a confusion has been made between an aggregation and an adsorption process. Our experiments show that a loss of ssDNA can occur at high pH, under conditions where dsDNA partitions entirely in the aqueous phase. We suspect that the original procedure used to isolate ϕX 174 ssDNA (phenol extraction in the presence of a saturated sodium tetraborate solution, [41]) as well as other commonly used procedures lead to a significant loss of ssDNA through adsorption, and we will investigate this issue elsewhere. Presumably, the loss of material only requires that a portion of the nucleic acids be single stranded; in addition, the percentage of lost (adsorbed) DNA is likely to increase with the dilution of the DNA in the aqueous phase. These two conditions (presence of ssDNA portions in dsDNA, low concentrations) are encountered when working with degraded dsDNA, for

instance, in forensic research or when one isolates ancient DNA. We will mention, as an example, the extraction of DNA from Neandertal femur (performed in the presence of 0.5 M Sodium EDTA, pH 8, [160]). It is possible that the extraction procedures that are presently used in these fields lead to an overlooked loss of nucleic acids. We hope that our results will help design better extraction protocols for such situations.

4.3.2 Implications for partitioning studies

Beyond the specific case of nucleic acids, our results have led us to examine the use of partition coefficients in the field of quantitative-structure-activity relationships (QSAR) [161]. Partition coefficients between water and an organic solvent (in particular octanol) are widely used to measure the hydrophobicity (or lipophilicity) of solutes. Typically, one measures the bulk solubility of the solute both in water and in the organic solvent to define its partition coefficient. These simple coefficients have proved to be of great value for the understanding of biological properties of the solute (such as biochemical, pharmaceutical, toxicological and environmental properties). Clearly, the behavior of the solute at the interface between the water and the organic phase is not taken into consideration in this approach. Our results show that in order to understand the biochemical properties of nucleic acids in a water-phenol two-phase system, the knowledge of the interfacial partitioning is absolutely required. It appears therefore that the knowledge of the interfacial behavior of a solute, in addition to the knowledge of its usual partition coefficient, should help to understand its biological properties.

4.4 Implications for the evolution of biological chemistry

The adsorption and renaturation of nucleic acids at interfaces is of interest for prebiotic chemistry. Indeed, one of the main problems of prebiotic chemistry today is to understand the synthesis and replication of the first polymeric chains, in the general context of a nucleic acid world. It raises a problem of polymerization, that was first formulated long ago in the context of a proteic prebiotic world. The basic concepts of heterogeneous chemistry have found applications here, with an emphasis on a surface chemistry of the liquid-solid interface [162]. We summarize the present knowledge in this field in the following sections.

4.4.1 Heterogeneous prebiotic chemistry

Condensation polymerization offers a plausible mechanism to explain the appearance of the first polymeric chains. However, bulk condensation polymerization reactions are known to be thermodynamically driven towards hydrolysis in dilute aqueous solutions, and also kinetically unfavorable if the concentration of monomers is low [61,64].

Thus, prebiotic chemistry is a field where the limitations of homogeneous chemistry have long been perceived. Note that the limits of bulk polymerization are also well known in polymer chemistry: both emulsion polymerization and heterophase polymerization are known to be more rapid and to lead to longer polymers than homogeneous polymerization does [163].

Two ideas borrowed from heterogeneous chemistry have been considered in great detail in prebiotic chemistry. The first one is Oparin's proposal of the role of coacervation. Coacervation is a liquid-liquid phase separation involving polymeric chains. Oparin favored the idea that prebiotic polymerization reactions took place in a heterogeneous, coacervated system, rather than in the bulk of a homogeneous phase [164]. Another suggestion made by Bernal [60] and other researchers [62,63,165] is that prebiotic polymerization reactions took place on the surface of minerals such as clays. The adsorption of the monomers on the surface would both increase their local concentration and lower their bulk state of hydration. The adsorption of nucleotides and amino acids at the liquid-solid interface of clays has been shown to lead to their extensive polymerization, providing support for this adsorption scenario [62].

4.4.2 Heterogeneous prebiotic chemistry in a nucleic acid world

Early ideas on the first replicating biopolymers promoted by Oparin and others focused on polypeptides [164]. Later one envisioned that the first self-replicating systems consisted of RNA and polypeptides [166]. More recently, the discovery that RNA could be endowed with catalytic properties [167] has stimulated the idea of an initial era where the replicating systems consisted essentially of nucleic acids [57–59]. Base-pairing processes (annealing and unwinding) are required in these systems, making nucleic acid helix-coil transitions on surfaces processes of great interest. In a general manner, the heterogeneous chemistry of nucleic acids should be at the heart of prebiotic chemistry, because one can use it for both polymerization and replication reactions. The coacervation scenario elaborated by Oparin is still relevant in a nucleic acid world, since coacervation of nucleic acids is also possible [168]. Interfacial scenarios involving liquid-liquid or liquid-solid interfaces are considered below.

4.4.3 Prebiotic chemistry: a role for phenol in a nucleic acid world

From our results and the analysis of the relevant literature, phenol emerges as an efficient compound in terms of its ability to interact single-stranded nucleic acids. We discuss now the implications of these findings for the evolution of biological catalysis.

Here is a list of arguments in favor of a role for phenol in a nucleic acid world.

1) Phenol is a plausible prebiotic compound

Phenol is known to be a plausible prebiotic compound: it can for instance be obtained from benzene, a compound present in interstellar matter (see [56] and further references therein).

2) Phenol binds efficiently to nucleic acids

The compounds active in a nucleic acids world are expected to be able to bind efficiently to nucleic acids. Phenol fulfills this requirement since it can interact with nucleic acids through aromatic interactions, not only in the bulk of an aqueous solution, but also at the interface between the water and the phenolic phases. Our results further show that phenol is the most efficient compound for this interfacial interaction among a variety of organic compounds.

We can apply the same reasoning on nucleic acid binding properties to the amino acids that can be obtained by prebiotic synthesis, which include the aromatic amino acids phenylalanine, tryptophan and tyrosine (see [169] for a review). We will mention here the results of a study of the interaction of immobilized amino acids with nucleotides [170]. The aromatic amino acids phenylalanine, tryptophan and tyrosine were the most efficient compounds among nine amino acids tested in these experiments (this clearly favors a common role of a stacking interaction). Remarkably, tyrosine had the highest affinity for the five nucleotides 5′-Up, 5′-Cp, 5′-Ip, 5′-Ap and 5′-Gp (where U, C, I, A and G indicate uridine, cytidine, inosine, adenosine and guanosine [170]: only tryptophan has a slightly better affinity for guanosine-5′-monophosphate). Thus, we conclude 1) that the remarkable affinity of the phenolic group for ssDNA reported here is also observed for the interaction of immobilized amino acids with nucleotides and 2) that the considerations on nucleic acids binding properties suggest an explanation for the later selection of aromatic amino acids among the twenty usual amino acids. In short, the phenol-nucleic acid interaction described here could have been a first step in the coevolution of nucleic acids and aminoacids.

3) Adsorption on a liquid-liquid interface: the oil-brine interface scenario

Clays and other mineral surfaces have been shown to promote the polymerization of amino acids and nucleotides. In these materials, the catalytic surface is a liquid-solid interface. We have seen above that a lack of fluidity in this interface is poorly compatible with an efficient surface diffusion. Such surfaces also lack the flexibility which is found in present-day enzymes, and which is known to be crucial to catalysis [171]. This leads us to consider another type of primitive catalyst, where the catalytic surface is a liquid-liquid interface: the surface of a droplet of oil in a salty aqueous medium. A similar interfacial origin of life involving the interface between an oil slick and salty water has been put forward by Onsager [65]. Onsager has shown that such an interfacial scenario has a number of attractive features such as possibility of interfacial polymerization, of accumulation of amphipathic molecules, creation of emulsion by mechanical agitation. A striking of this feature of an oil-brine interfacial scenario is that "*does not require an initial capability to synthesize the constituents of the cell envelopes as well as the macromolecules needed for catalysis and replication*" [65]. This suggests that this type of scenario should contribute to our understanding of the origin of membranes in a prebiotic world [172,173]. Let us note also that the likening of an enzyme with an oil droplet is not new: Perutz [174] has observed for instance that: "*the non-polar interior of enzymes provides the living cell with the equivalent of the organic solvents used by the chemists*". Our point of view is somewhat different from the point of view of Perutz because we emphasize the interfacial properties of the oil droplet. Furthermore, the proposal that we want to make here concerns specifically the organic solvent that we consider, namely phenol, and appears therefore as a refinement of Onsager's proposal.

4) Phenol droplets have a key catalytic activity

Phenol droplets have an annealing catalytic activity as shown by Kohne *et al.* [1] and here. Furthermore, this annealing activity has been reported for both ribonucleic acids and DNA [1]. It has been stressed that an important obstacle to the self-replication of nucleic acids is the presence of intramolecular stable structures [58,175]. Phenol could clearly help solve this problem. Thus, phenol has not only the expected binding properties but also a key required chaperone catalytic property. In addition, the release of dsDNA from the water-phenol after renaturation allows the reaction to turnover as mentioned before.

5) Phenol droplets can be generated in hydrothermal systems

Geochemical and microbiological evidence favor the hypothesis that early life has evolved near hydrothermal systems, at high temperatures (about 100 °C). A temperature of about 100 °C is in the typical range of the critical solution temperature in a brine-phenol mixture [77], and this raises the possibility of using heating and cooling cycles of brine-phenol mixtures above and below this temperature could have been used to produce large amounts of small phenolic droplets. Recently, Braun and Libchaber [176] have shown that thermal gradient can be used to increase the local concentration of DNA, and pointed out the relevance of this finding to the problem of prebiotic chemistry. There are interesting connections between the thermophoretic effect they describe and the mechanism that we propose for generating phenol droplets. In both cases, we obtain a large increase of the local concentration of nucleic acids, and this increase involves a convective effect rather than simple diffusion. The concentrating mechanism proposed by Braun and Libchaber [176] and the adsorption process

envisioned here do not exclude one another, and could have operated simultaneously.

6) **The chemistry of phenol could have been used in a nucleic acid world**

The phenolic group is known to offer numerous possibilities in organic chemistry. The chemistry of phenol and of phenolic compounds could also have been exploited in a nucleic acid world. The ability of phenolic compounds to capture light energy suggests for instance that phenol or simple phenolic groups could have been used as early pigments, thus contributing to solve bioenergetic problems associated with prebiotic evolution [177]. The linking of phenol to nucleic acids could also have been used to expand the catalytic properties of ribozymes: Robertson and Miller [56] have explored this possibility, and shown that a variety of nucleophiles, including phenol, can become bound to 5-hydroxymethyluracil under prebiotic conditions.

7) **Phenol is ubiquitous in present-day biochemistry**

A last argument comes from the ubiquity of phenol and phenolic compounds (such as tyrosine) in present-day biochemistry. Ubiquity would reflect phenol's antiquity. Several of the reactions involving phenol or phenolic groups today appear to be of interest from the point of view of prebiotic chemistry. The uibquinol/ubiquinone system for instance could be the relic of the early pigments mentioned above.

All these considerations lead us to propose that phenol droplets can catalyze the formation of polynucleotides under appropriate conditions; we hope that this hypothesis will soon be tested. An attractive feature of the phenol-brine two-phase system is that it should be possible to anchor any type of catalyst at the interface, provided it can be covalently linked to a single-stranded nucleic acid chain that can be adsorbed at the interface. While we believe that such interfacial catalysis could take place in a simple water-phenol system, we wish to point out that a simultaneous role of solid catalysts such as clays could also be tested. Indeed, clays are well known for their capacity to absorb phenolic compounds (this is a major theme in humus chemistry, see [178] and further references therein), and it may also be the case that the presence of phenol increase the efficiency of clay-catalyzed polymerization [62].

4.4.4 Early stages of life: a role for phenol in hyperthermophiles

In the preceding section, we provided plausible arguments in favor of a role of phenol in prebiotic chemistry. More direct evidence can be offered at the later stage corresponding to the appearance of archaebacteria. Hyperthermophiles are considered to be closely related to the earliest forms of archaebacteria [179]. The hyperthermophile *Ferroglobus placidus* can grow at 85 °C using phenol as the sole electron donor [180]. Furthermore, the growth oc-

curred in anaerobic conditions and using Fe(III) as the electron acceptor. These three features (use of simple aromatic compounds present in the deep, hot subsurface [181, 182], anaerobic growth and the use of Fe(III)) [183]) are thought to have been important processes on the early Earth. Thus, these experiments provide a more direct support in favor of the role of phenol during the appearance of archaebacteria.

4.4.5 Some remarks on the functions of phenol in present-day biochemistry

Our proposal that phenol played a key role in the origin of life may seem paradoxical if one recalls that phenol is well known as an antiseptic and a toxic compound. However, it must be stressed that the present-day biochemistry need not bear a deep resemblance with prebiotic chemistry. The efficiency of phenol as an antiseptic varies with cell types: phenol is more toxic to eukaryotic cells such as leukocytes than to bacterial cells such as staphylococci or streptococci [184]. The toxicity of phenol varies also greatly among bacterial cells (as discussed above, some extremophiles can grow on phenol at concentrations and temperatures that would be lethal to eubacteria). The same type of observations can be made concerning the ability of phenol to act as a denaturant. While many enzymes are denatured by phenol, there are reports of resistance to denaturation, for instance in the case of RNase, whose catalytic activity can withstand phenol extraction [159]. Another example concerns the DNA polymerase of *Thermus thermophilus*, which retains its catalytic properties in the presence of several percent phenol at 55–65 °C [185]). A similar observation can be made on the peptidyl transferase activity of ribosomes [186]. The catalytic activity is performed by a ribozyme [187]. *Escherichia coli* ribosomes lose this activity upon phenol extraction; in contrast the ribosomes of the thermophilic eubacterium *Thermus aquaticus* retain 80% of this activity after treatment with proteinase K and SDS followed by vigorous extraction with phenol [186]. All these experiments raise the possibility that the first catalysts (ribozymes or enzymes) had a resistance to the denaturing action of phenol that has been progressively lost in the course of evolution. As explained above, such catalysts can be anchored at the brine-phenol interface through a fusion with an appropriate single-stranded nucleic acid chain, opening the possibility of developing an interfacial catalysis in this system.

It is also important to note here that there are very few investigations dealing with the interactions of phenol with polypeptides. One of the reasons explaining the avoidance of phenol in denaturation studies is that it absorbs UV light and prevents the standard use of UV spectroscopy to monitor unfolding. The comprehensive review of Singer [188] on the properties of proteins in nonaqueous solvents makes no mention of experiments involving phenol. More recently, Zaks and Klibanov have performed striking experiments, showing that a number of enzymes are active in a variety of organic solvents [189,190]. Phenol

was again not among the solvents tested. Clearly, there is room for additional work in this field.

5 Summary and concluding remarks

5.1 Summary of the experimental results

We examined the room temperature behavior of very dilute solutions of two complementary 118 base-long single-stranded DNA chains in a two-phase system containing water, phenol and sodium chloride. 1) In the absence of its complementary strand, each single-stranded DNA chain can be adsorbed to the water-phenol interface in a salt-dependent manner. At 0.85 M NaCl, 80% of the chains are irreversibly adsorbed. In the absence of shaking, this adsorption is a slow, monomolecular, diffusion-controlled process. The adsorption is completed within a few seconds if the solution is vigorously shaken. In addition to phenol, we tested thirteen other organic solvents for their ability to adsorb single-stranded DNA at the water-solvent interface. Phenol is the most efficient solvent, followed by other planar aromatic compounds. This supports a role for phenol stacking in its interaction with single-stranded DNA. 2) The addition of a single-stranded chain in a brine-phenol two-phase system (0.85 M NaCl) where the complementary single-strand has been previously adsorbed initiates an interfacial renaturation reaction, coupled to the release of the renatured double-stranded DNA in the aqueous phase. In the absence of shaking, the adsorption of this added single-strand and DNA renaturation occur at similar rates at short time. At longer time a Langmuir-Hinshelwood process requiring a two-dimensional diffusion of the complementary chains is involved in their reassociation. 3) The addition of the two complementary chains in the aqueous phase of this brine-phenol system followed by a constant, vigorous shaking leads to a fast interfacial renaturation. We have determined a bimolecular rate of renaturation equal to $4.2 \pm 0.4 \times 10^{10}\,\mathrm{M^{-1}s^{-1}}$; this rate greatly exceeds the Smoluchowski limit for a three-dimensional diffusion-controlled reaction.

5.2 Summary of the discussion

The present investigation has been inspired by the work of Kohne, Levison and Myers on the Phenol Emulsion Reassociation Technique or PERT. Our results show that for very low DNA concentrations, PERT is an interfacial reaction. The existence of a coupling between adsorption and renaturation accounts for the unusual salt dependence of the reaction. A comparison of PERT with other approaches used to obtain high renaturation rates (involving either simple DNA condensing agents or single-stranded nucleic acid binding proteins) shows that PERT is the most efficient technique and reveals similarities between PERT and the renaturation reaction performed by single-stranded nucleic acid binding proteins. The most efficient renaturation reactions (in the presence of condensing agents or with PERT) do not occur in the bulk of

a homogeneous phase. Rather, they belong to the field of heterogeneous chemistry. We clarified the connection between standard concepts of surface chemistry (Eley-Rideal and Langmuir-Hinshelwood mechanisms) and the work on reduction of dimensionality of Adam and Delbrück. We have seen that fluid interfaces allow efficient surface diffusion processes through an interface-assisted mobility, which is expected to lead to a Rouse mobility for adsorbed polymeric chains. Our results also lead to a better understanding of the partitioning of nucleic acids in two-phase systems, and should help design improved extraction procedures for damaged nucleic acids. Beyond the specific case of nucleic acids, partitioning studies are at the heart of quantitative structure-activity studies; the emphasis in these studies has generally been the measurements of the bulk solubility of a given solute in water and an organic solvent. Our results show that these studies should be benefit from a knowledge of the behavior of this solute at the interface between water and this organic solvent. We discussed the role of phenol, liquid-liquid interfaces and convection from the point of view of prebiotic chemistry and today biochemistry. We reached the conclusion that phenol and phenol droplets could have played a central role both in prebiotic chemistry and in the early stages of life, refining ideas of Onsager on an oil-brine interfacial origin of life. This work highlights the importance of aromaticity in molecular biology. On the whole, it fully supports the intuitions of Kohne, Levison and Byers about the physiological interest of PERT, as well as about its prebiotic significance.

5.3 Concluding remarks

5.3.1 Homogeneous and heterogeneous biochemistry of nucleic acids

The current description of nucleic acid biochemistry is mainly based on *in vitro* experiments performed in the bulk of homogeneous, dilute aqueous solutions [92,191–194]. In chemistry, the investigation of chemical reactions distinguishes between homogeneous chemistry, where the reaction proceeds in the bulk of a homogeneous phase, and heterogeneous chemistry, where the reaction involves more than one phase. In the same manner, one can draw a distinction between homogeneous biochemistry and heterogeneous biochemistry. Clearly, the current description of nucleic acid biochemistry is mainly based on homogeneous biochemistry. In contrast, we have shown here that the most efficient renaturation reactions pertain to heterogeneous biochemistry. Furthermore, our study of the water-phenol interfacial renaturation reveals striking similarities with the catalysis by SSBPs. This implies that homogenous approaches in nucleic acid biochemistry have limitations, and that the study of heterogeneous system should lead to a better understanding of the behavior of nucleic acids, both *in vitro* and *in vivo*. We will examine this issue elsewhere.

References

1. D.E. Kohne, S.A. Levison, M.J. Byers, Biochemistry **16**, 5329 (1977).
2. R. Wieder, J.G. Wetmur, Biopolymers **21**, 665 (1982).
3. J.-L. Sikorav, G.M. Church, J. Mol. Biol. **222**, 1085 (1991).
4. L.M. Kunkel *et al.*, Proc. Natl. Acad. Sci. U.S.A. **82**, 4778 (1985).
5. S.A. Chow, C.M. Radding, Proc. Natl. Acad. Sci. U.S.A. **82**, 5646 (1985).
6. G. Vesnaver, K.J. Breslauer, Proc. Natl. Acad. Sci. U.S.A. **88**, 3569 (1991).
7. J.A. Holbrook *et al.*, Biochemistry **38**, 8409 (1999).
8. I. Chaperon, J.-L. Sikorav, Biopolymers **46**, 195 (1998).
9. W. Kauzmann, Adv. Protein Chem. **14**, 1 (1959).
10. L. Levine, J.A. Gordon, W.P. Jencks, Biochemistry **2**, 168 (1963).
11. P.O.P. Ts'o, G.K. Helmkamp, C. Sander, Proc. Natl. Acad. Sci. U.S.A. **48**, 686 (1962).
12. F. Helmer, K. Kiehs, C. Hansch, Biochemistry **7**, 2858 (1968).
13. P.O.P. Ts'o, I.S. Melvin, A.C. Olson, J. Am. Chem. Soc. **85**, 1289 (1963).
14. P.O.P. Ts'o, in *Basic Principles in Nucleic Acid Chemistry*, edited by P.O.P. Ts'o, Vol. **1** (Academic Press, New York, 1974) p. 453.
15. R.C. Davis, I. Tinoco Jr., Biopolymers **6**, 223 (1968).
16. P.H. von Hippel, T. Schleich, in *Structure and Stability of Biological Macromolecules*, edited by S.N. Timasheff, G.D. Fasman (Marcel Dekker, Inc., New York, 1969) p. 417.
17. T.T. Herskovits, J.P. Harrington, Biochemistry **11**, 4800 (1972).
18. M. Leng *et al.*, Biochimie **56**, 887 (1974).
19. J.C. Ma, D.A. Dougherty, Chem. Rev. **97**, 1303 (1997).
20. J. Marmur, P. Doty, J. Mol. Biol. **3**, 585 (1961).
21. D. Pörschke, M. Eigen, J. Mol. Biol. **62**, 361 (1971).
22. M.E. Craig, D.M. Crothers, P. Doty, J. Mol. Biol. **62**, 383 (1971).
23. F.W. Studier, J. Mol. Biol. **41**, 199 (1969).
24. J.G. Wetmur, N. Davidson, J. Mol. Biol. **31**, 349 (1968).
25. B.W. Pontius, P. Berg, Proc. Natl. Acad. Sci. U.S.A. **88**, 8237 (1991).
26. B.M. Alberts, L. Frey, Nature **227**, 1313 (1970).
27. G.M. Weinstock, K. McEntee, I.R. Lehman, Proc. Natl. Acad. Sci. U.S.A. **76**, 126 (1979).
28. C. Christiansen, R.L. Baldwin, J. Mol. Biol. **115**, 441 (1977).
29. J.E. Rothman, R.D. Kornberg, Nature **322**, 209 (1986).
30. S.C. Kowalczykowski, A.K. Eggleston, Annu. Rev. Biochem. **63**, 991 (1994).
31. T.M. Lohman, M.E. Ferrari, Annu. Rev. Biochem. **63**, 527 (1994).
32. Z. Tsuchihashi, P.O. Brown, J. Virol. **68**, 5863 (1994).
33. D. Herschlag, J. Biol. Chem. **270**, 20871 (1995).
34. C. Gabus *et al.*, J. Biol. Chem. **276**, 19301 (2001).
35. E.A. DiMarzio, M. Bishop, Biopolymers **13**, 2331 (1974).
36. G.A. Carri, M. Muthukumar, Phys. Rev. Lett. **82**, 5405 (1999).
37. M.G. Sevag, D.B. Lackman, J. Smolens, J. Biol. Chem. **124**, 425 (1938).
38. A. Gierer, G. Schramm, Nature **177**, 702 (1956).
39. K.S. Kirby, Biochem. J. **64**, 405 (1956).
40. K.S. Kirby, Biochem. J. **66**, 495 (1957).
41. R.L. Sinsheimer, J. Mol. Biol. **1**, 43 (1959).
42. J. Marmur, J. Mol. Biol. **3**, 208 (1961).
43. J. Sambrook, E.F. Fritsch, T. Maniatis, *Molecular Cloning. A Laboratory Manual*, second ed. (Cold Spring Harbor Laboratory Press, New York, 1989).
44. P.-Å. Albertsson, *Partition of Cell Particles and Macromolecules* (John Wiley and Sons, New York, 1960).
45. H. Walter, D.E. Brooks, D. Fisher, *Partitioning in Aqueous Two-Phase Systems. Theory, Methods, Uses, and Applications to Biotechnology* (Academic Press, Inc., Orlando, 1985).
46. A. Pusztai, Biochem. J. **99**, 93 (1966).
47. H. Saito, K.-I. Mura, Biochim. Biophys. Acta **72**, 619 (1963).
48. H.R. Massie, B.H. Zimm, Proc. Natl. Acad. Sci. U.S.A. **54**, 1641 (1965).
49. M. Zasloff, G.D. Ginder, G. Felsenfeld, Nucleic Acids Res. **5**, 1139 (1978).
50. D. Müller *et al.*, Biochim. Biophys. Acta **740**, 1 (1983).
51. R.P. Perry *et al.*, Biochim. Biophys. Acta **262**, 220 (1972).
52. M. Piechowska, D. Shugar, Acta Biochim. Pol. **10**, 263 (1963).
53. M. Piechowska, D. Shugar, Acta Biochim. Pol. **12**, 11 (1965).
54. T.I. Tikhonenko, G.A. Perevertailo, S.P. Vorotilo, Biochemistry (Moscow) **31**, 197 (1966).
55. D.M. Skinner, L.L. Triplett, Biochem. Biophys. Res. Co. **28**, 892 (1967).
56. M.P. Robertson, S.L. Miller, Science **268**, 702 (1995).
57. W. Gilbert, Nature **319**, 618 (1986).
58. G.F. Joyce, Nature **338**, 217 (1989).
59. G. Joyce, Nature **418**, 214 (2002).
60. J.D. Bernal, *The Physical Basis of Life* (Routledge and Kegan Paul, London, 1951).
61. N.R. Pace, Cell **65**, 531 (1991).
62. J.P. Ferris *et al.*, Nature **381**, 59 (1996).
63. S.J. Sowerby *et al.*, Proc. Natl. Acad. Sci. U.S.A. **98**, 820 (2001).
64. G. Zubay, *Origins of Life on the Earth and in the Cosmos*, 2nd ed. (Academic Press, San Diego, 2000).
65. L. Onsager, in *Quantum Statistical Mechanics in the Natural Sciences*, edited by S.L. Mintz, S.M. Widmayer (Plenum Press, New York, Coral Gables, 1974) p. 1.
66. F. Sanger *et al.*, J. Mol. Biol. **125**, 225 (1978).
67. A.F.H. Ward, L. Tordai, J. Chem. Phys. **14**, 453 (1946).
68. J. Crank, *The Mathematics of Diffusion*, 2nd ed. (Clarendon Press, Oxford, 1975).
69. D. Lang, P. Coates, J. Mol. Biol. **36**, 137 (1968).
70. C.N. Hinshelwood, *The Kinetics of Chemical Change* (The Clarendon Press, Oxford, 1940).
71. A. Zangwill, *Physics at Surfaces* (Cambridge University Press, Cambridge, 1988).

72. J.C. Jaeger, Philos. Mag. **32**, 324 (1941).
73. N.Y. Ölçer, Q. Appl. Math. **26**, 335 (1968).
74. H.S. Carslaw, J.C. Jaeger, *Conduction of Heat in Solids* (Oxford University Press, Oxford, 1959).
75. H.C. Berg, E.M. Purcell, Biophys. J. **20**, 193 (1977).
76. V.G. Levich, *Physicochemical Hydrodynamics* (Prentice-Hall, Englewood Cliffs, 1962).
77. J. Timmermans, Z. Phys. Chem. **58**, 129 (1907).
78. E. von Schürmann, R. Diederichs, Ber. Bunseng. Ges. Phys. Chem. **68**, 434 (1964).
79. A.E. Hill, W.M. Malisoff, J. Am. Chem. Soc. **48**, 918 (1926).
80. A.N. Campell, A.J.R. Campell, J. Am. Chem. Soc. **59**, 2481 (1937).
81. Z.X. Li *et al.*, J. Phys. Chem. B **102** (1998).
82. F.H. Rhodes, A.L. Markley, J. Phys. Chem. **25**, 527 (1921).
83. B. von Meuthen, M. Stackelberg, Z. Elektrochem. **64**, 387 (1960).
84. J. Duckett, W.H. Patterson, J. Phys. Chem. **29**, 259 (1925).
85. J.H. Carrington, L.R. Hickson, W.H. Patterson, J. Chem. Soc. **127**, 2544 (1925).
86. P. Hagenmuller, A. Lecerf, C.R. Hebd. Séances Acad. Sci. **245**, 1546 (1957).
87. E. Papafil, M.-A. Papafil, C. Beldie, Analele stiint univ "Al. I. Cuza" Iasi Sect I **4**, 153 (1958).
88. B. Belhachemi, A.A. Gotouk, J. Chim. Phys. **96**, 1186 (1999).
89. Wagner, Z. Phys. Chem. **132**, 273 (1928).
90. I. Prigogine, Bull. Soc. Chim. Belg. **52**, 115 (1943).
91. J.L. Meijering, Philips Res. Rep. **5**, 333 (1950).
92. M.T. Record Jr., C.F. Anderson, T.M. Lohman, Q. Rev. Biophys. **11**, 103 (1978).
93. G.S. Manning, Q. Rev. Biophys. **11**, 179 (1978).
94. B.E. Conway, J.A.V. Butler, J. Chem. Soc., 3075 (1952).
95. J.D. Mandell, A.D. Hershey, Anal. Biochem. **1**, 66 (1960).
96. J.F. Escara, J.R. Hutton, Biopolymers **19**, 1315 (1980).
97. S.M. Mel'nikov *et al.*, J. Am. Chem. Soc. **121**, 1130 (1999).
98. S.B. Smith, Y. Cui, C. Bustamante, Science **271**, 795 (1996).
99. F.W. Studier, J. Mol. Biol. **41**, 189 (1969).
100. A. Schaper, C. Urbanke, G. Maass, J. Biomol. Struct. Dyn. **6**, 1211 (1991).
101. A.R. Wolfe, T. Meehan, Nucleic Acids Res. **22**, 3147 (1994).
102. P. Debye, *Polar Molecules* (The Chemical Catalog Company, Inc, New York, 1929).
103. J.E. Hearst, Biopolymers **3**, 57 (1965).
104. E. Westhof, Annu. Rev. Biophys. Biophys. Chem. **17**, 125 (1988).
105. *DNA hydration*, Biopolymers, Nucleic Acid Science **48** (4), special issue (1998).
106. H. Eisenberg, G. Felsenfeld, J. Mol. Biol. **30**, 17 (1967).
107. D.R. Lide (Editor), *CRC Handbook of Chemistry and Physics* (CRC Press, Boca Raton, 2003).
108. W. Saenger, *Principles of Nucleic Acid Structure* (Springer Verlag, New York, 1984).
109. J.D. Bernal, R. Fowler, J. Chem. Phys. **1**, 515 (1933).
110. S. Neidle, H.M. Berman, H.S. Shieh, Nature **288**, 129 (1980).
111. W. Saenger, C. Betzel, Nature **296**, 581 (1982).
112. L.S. Lerman, J. Mol. Biol. **3**, 18 (1961).
113. P.G. de Gennes, *Scaling Concepts in Polymer Physics* (Cornell University Press, Ithaca, 1979).
114. P.G. de Gennes, J. Phys. (Paris) **37**, 1445 (1976).
115. M. Joanicot, B. Revet, Biopolymers **26**, 315 (1987).
116. J. Brahms, A.M. Michelson, K.E. van Holde, J. Mol. Biol. **15**, 467 (1966).
117. J.G. Wetmur, Crit. Rev. Biochem. Mol. Biol. **26**, 227 (1991).
118. M. von Smoluchowski, Z. Phys. Chem. **92**, 129 (1917).
119. J. Marmur, R. Rownd, C.L. Schildkraut, in *Progress in Nucleic Acid Research*, edited by J.N. Davidson, W.E. Cohn, Vol. **1** (Academic Press, New York, 1963) p. 231.
120. M. Eigen, in *Nobel Symposium in Fast Reactions and Primary Processes in Chemical Kinetics, Stockholm, 1967*, edited by S. Claesson, Vol. **5** (Almqvist and Wiksell, Stockholm, 1967) p. 333.
121. B. Duplantier, G. Jannink, J.-L. Sikorav, in *Slow Dynamical Processes in Heterogeneous Soft Matters, Les Houches, 1995*, edited by J.-P.C. Addad, A. Guillermo, A. Viallat, D. Bordeaux (Centre de Physique des Houches, Les Houches, 1995) p. 55.
122. T.C. Laurent, B.N. Preston, B. Carlsson, Eur. J. Biochem. **43**, 231 (1974).
123. H. Tabor, Biochemistry **1**, 496 (1962).
124. K. Morimatsu, M. Takahashi, Adv. Biophys. **31**, 23 (1995).
125. R.A. Anderson, J.E. Coleman, Biochemistry **14**, 5485 (1975).
126. Y. Shamoo *et al.*, Nature **376**, 362 (1995).
127. S. Raghunathan *et al.*, Nature Struct. Biol. **7**, 648 (2000).
128. T. Hollis *et al.*, Proc. Natl. Acad. Sci. U.S.A. **98**, 9557 (2001).
129. R. Romer *et al.*, Biochemistry **23**, 6132 (1984).
130. S.S. Tsang, S.A. Chow, C.M. Radding, Biochemistry **24**, 3226 (1985).
131. S.P. Stoylov *et al.*, Biopolymers **41**, 301 (1997).
132. W.C. Williams *et al.*, Proc. Natl. Acad. Sci. U.S.A. **98** (2001).
133. P.K. Nandi, P.Y. Sizaret, Arch. Virol. **146**, 327 (2001).
134. G.G. Hammes, A.C. Park, J. Am. Chem. Soc. **90**, 4151 (1968).
135. M. Eigen, L. DeMaeyer, Z. Elektrochem. **59**, 986 (1955).
136. R.B. Bird, W.E. Stewart, I.N. Lightfoot, *Transport Phenomena*, 2nd ed. (John Wiley, New York, 2002).
137. J. Widom, R.L. Baldwin, Biopolymers **22**, 1595 (1983).
138. M. Hegner, S.B. Smith, C. Bustamante, Proc. Natl. Acad. Sci. U.S.A. **96**, 10109 (1999).
139. D.R. Ripoll *et al.*, Proc. Natl. Acad. Sci. U.S.A. **90**, 5128 (1993).
140. K. Nadassi, S.J. Wodak, J. Janin, Biochemistry **38**, 1999 (1999).
141. E.B. Zhulina, T.M. Birshtein, A.M. Skvortsov, Biopolymers **19**, 805 (1980).
142. A.Y. Grosberg, Biophysics-USSR **29**, 621 (1984).
143. J.E. Lennard-Jones, Proc. Phys. Soc. **49**, 140 (1937).
144. N.K. Adam, *The Physics and Chemistry of Surfaces*, third ed. (Oxford University Press, Oxford, 1941).
145. G. Adam, M. Delbrück, in *Structural Chemistry and Molecular Biology*, edited by A. Rich, N. Davidson (W.H. Freeman & Company, San Francisco, 1968) p. 198.
146. D. Wang, S.-Y. Gou, D. Axelrod, Biophys. Chem. **43**, 117 (1992).

147. V. Chan, D.J. Graves, S.E. Mckenzie, Biophys. J. **69**, 2243 (1995).
148. S.A. Sukhishvili *et al.*, Macromolecules **35**, 1776 (2002).
149. M. Guthold *et al.*, Biophys. J. **77**, 2284 (1999).
150. B. Maier, J.O. Rädler, Phys. Rev. Lett. **82**, 1911 (1999).
151. B. Maier, J.O. Rädler, Macromolecules **33**, 7185 (2000).
152. A.D. Riggs, S. Bourgeois, M. Cohn, J. Mol. Biol. **53**, 401 (1970).
153. P.H. Richter, M. Eigen, Biophys. Chem. **2**, 255 (1974).
154. O.G. Berg, R.B. Winter, P.H. von Hippel, Biochemistry **20**, 6929 (1981).
155. R.B. Winter, O.G. Berg, P.H. von Hippel, Biochemistry **20**, 6961 (1981).
156. W. Grassmann, G. Deffner, Hoppe Seylers Z. Physiol. Chem. **293**, 89 (1953).
157. K.S. Kirby, Biochem. J. **36**, 117 (1959).
158. J.M. Chirgwin *et al.*, Biochemistry **27**, 5294 (1979).
159. P. Chomczynski, N. Sacchi, Anal. Biochem. **162**, 156 (1987).
160. M. Krings *et al.*, Cell **90**, 19 (1997).
161. A. Leo, C. Hansch, D. Elkins, Chem. Rev. **71**, 525 (1971).
162. N. Lahav, Heterogen. Chem. Rev. **1**, 159 (1994).
163. P.J. Flory, *Principles of Polymer Chemistry* (Cornell University Press, Ithaca, 1953).
164. A.I. Oparin, Adv. Enzymol. **27**, 347 (1965).
165. M. Paecht-Horowitz, J. Berger, A. Katchalsky, Nature **228**, 636 (1970).
166. M. Eigen, Naturwissenschaften **58**, 465 (1971).
167. T.R. Cech, B.L. Bass, Annu. Rev. Biochem. **55**, 599 (1986).
168. J. Pelta, F. Livolant, J.-L. Sikorav, J. Biol. Chem. **271**, 5656 (1996).
169. S.L. Miller, Cold Spring Harb. Symp. Quant. Biol. **52**, 17 (1987).
170. C. Saxinger, C. Ponnamperuma, C. Woese, Nature New Biol. **234**, 172 (1971).
171. D.E. Koshland Jr., Cold Spring Harb. Symp. Quant. Biol. **52**, 1 (1987).
172. P. Mitchell, in *The Origin of Life on Earth*, edited by A.I. Oparin (Pergamon, London, Moscow, 1959) p. 437.
173. J.W. Szostak, D.P. Bartel, P.L. Luisi, Nature **409**, 387 (2001).
174. M. Perutz, Proc. R. Soc. London, Ser. B **167**, 349 (1967).
175. G.F. Joyce, L.E. Orgel, J. Mol. Biol. **188**, 433 (1986).
176. D. Braun, A. Libchaber, Phys. Rev. Lett. **89**, 188103 (2002).
177. D.W. Deamer, Microbiol. Mol. Biol. R. **61**, 239 (1997).
178. B.S. Xing *et al.*, Environ. Sci. Technol. **28**, 466 (1994).
179. C.R. Woese, Microbiol. Rev. **51**, 221 (1987).
180. J.M. Tor, D.R. Lovley, Environ. Microbiol. **3**, 281 (2001).
181. T. Gold, Proc. Natl. Acad. Sci. U.S.A. **89**, 6045 (1992).
182. N.R. Pace, Science **276**, 734 (1997).
183. M. Vargas *et al.*, Nature **395**, 65 (1998).
184. A. Fleming, Proc. R. Soc. London, Ser. B **96**, 171 (1924).
185. H.L. Katcher, I. Schwartz, Biotechniques **16**, 84 (1994).
186. H.F. Noller, V. Hoffarth, L. Zimniak, Science **256**, 1416 (1992).
187. P. Nissen *et al.*, Science **289**, 920 (2000).
188. S.J. Singer, Adv. Protein Chem. **17**, 1 (1962).
189. A. Zaks, A.M. Klibanov, J. Biol. Chem. **263**, 3194 (1988).
190. A. Zaks, A.M. Klibanov, J. Biol. Chem. **263**, 8017 (1988).
191. G. Felsenfeld, H.T. Miles, Annu. Rev. Biochem. **36**, 407 (1967).
192. V.A. Bloomfield, D.M. Crothers, I. Tinoco Jr., *Physical Chemistry of Nucleic Acids* (Harper and Row, New York, 1974).
193. C.R. Cantor, P.R. Schimmel, *Biophysical Chemistry. Part III. The Behavior of Biological Macromolecules* (W.H. Freeman and Company, New York, 1980).
194. V.A. Bloomfield, D.M. Crothers, I. Tinoco Jr., *Nucleic Acids. Structure, Properties and Functions* (University Science Books, Sausalito, 2000).